

UniRec-0.1B: Unified Text and Formula Recognition with 0.1B Parameters

Yongkun Du¹, Zheneng Chen^{1,†}, Yazhen Xie¹, Weikang Bai¹, Hao Feng², Wei Shi²,
 Yuchen Su¹, Can Huang², Yu-Gang Jiang^{1,†}

¹Fudan University, ²ByteDance

Abstract

Text and formulas constitute the core informational components of many documents. Accurately and efficiently recognizing both is crucial for developing robust and generalizable document parsing systems. Recently, vision-language models (VLMs) have achieved impressive unified recognition of text and formulas. However, they are large-sized and computationally demanding, restricting their usage in many applications. In this paper, we propose UniRec-0.1B, a unified recognition model with only 0.1B parameters. It is capable of performing text and formula recognition at multiple levels, including characters, words, lines, paragraphs, and documents. To implement this task, we first establish UniRec40M, a large-scale dataset comprises 40 million text, formula and their mix samples, enabling the training of a powerful yet lightweight model. Secondly, we identify two challenges when building such a lightweight but unified expert model. They are: structural variability across hierarchies and semantic entanglement between textual and formulaic content. To tackle these, we introduce a hierarchical supervision training that explicitly guides structural comprehension, and a semantic-decoupled tokenizer that separates text and formula representations. Finally, we develop a comprehensive evaluation benchmark covering Chinese and English documents from multiple domains and with multiple levels. Experimental results on this and public benchmarks demonstrate that UniRec-0.1B outperforms both general-purpose VLMs and leading document parsing expert models, while achieving a 2-9 \times speedup, validating its effectiveness and efficiency.

Correspondence: zhinchen@fudan.edu.cn, ygj@fudan.edu.cn

Codebase and Dataset: <https://github.com/Topdu/OpenOCR>

1 Introduction

Document parsing [72] serves as a key component in real-world applications like document understanding, digital education, and information retrieval, etc. As the core tasks of document parsing, text and formula recognition have traditionally been addressed as distinct tasks, each with extensive research [3, 14–16, 19, 29, 37, 47–49, 58, 68, 71] and significant progress over the past decades.

Recent advances in vision-language models (VLMs) [2, 8, 22, 25, 54, 65, 66, 78] have given rise to a paradigm of end-to-end document parsing [4, 6, 7, 9, 28, 30, 34, 39, 41, 42, 46, 62, 63], which demonstrate a remarkable ability to unify multiple modalities, such as text, formulas, tables, and charts, within a single framework. Although such unified approaches are conceptually elegant and demonstrate impressive performance, they typically depend on models with billions of parameters, leading to high computational costs and significant

[†]Corresponding authors.

inference latency. On the other hand, text and formulas constitute the dominant content in most documents. For instance, in OmniDocBench [44], text and formulas together account for 97.43% of page regions in quantity and 87.90% of the total parsing time by using MinerU2.5 [42], as shown in Fig. 1. This observation suggests that improving the efficiency of text and formula recognition is crucial for document parsing acceleration. Motivated by this, we introduce UniRec-0.1B, a lightweight recognition model with only 0.1 billion parameters. We aim at using this model to jointly recognize textual and formula content across multiple levels (e.g., character, word, line, and paragraph), and thus significantly improving the efficiency of document parsing. However, the first challenge encountered is training data. Existing datasets are limited in both scale and diversity, making it difficult for small models to achieve comprehensive learning in multi-task and multi-level settings. To address this, we first construct a large-scale Chinese and English text-formula recognition dataset including 40 million samples. The dataset integrates public text recognition data, Wikipedia articles, and LaTeX formulas extracted from arXiv papers. It covers a wide range of real-world scenarios such as digital-born documents, photographs, scanned pages, and handwritten content. This provides a solid data foundation for unified recognition.

Subsequently, achieving unified recognition by using such a small parameter budget raises two technical challenges. First, **structural variability**: Document elements across different levels exhibit significant structural diversity, making it difficult for the model to adapt to multi-granularity representations simultaneously. Second, **semantic entanglement**: Existing approaches typically employ a coupled tokenizer to process both text and formula modalities, where the same token may represent distinct semantics in purely text versus formula contexts. This coupling leads to semantic entanglement between modalities. While large language models (LLMs) can partially absorb such ambiguity through their huge model capacity, small models are far more sensitive to it, resulting in significant performance degradation.

To overcome these challenges, we introduce two novel techniques: Hierarchical Supervision Training (HST) and Semantics-Decoupled Tokenizer (SDT). HST explicitly inserts hierarchical tokens into the label sequence. They guide the model in recognizing and distinguishing different structural levels, thereby enhancing its ability to model hierarchical structures. SDT constructs independent vocabularies for textual and formula modalities, fundamentally eliminating the cross-modality semantic confusion.

To evaluate the performance of UniRec-0.1B comprehensively, we build UniRec-Bench, a benchmark of Chinese and English documents covering text, formula, text-formula mixed content with multiple levels and domains based on OmniDocBench [44]. Experimental results demonstrate that UniRec-0.1B achieves highly competitive accuracy compared to large-scale VLM-based document parsing models [4, 6, 7, 9, 28, 30, 34, 39, 41, 46, 62, 63] on various text and formula recognition tasks. Furthermore, by replacing the recognition modules of existing document parsing models with UniRec-0.1B, 2-9× overall parsing speedup is observed. These results highlight the effectiveness of UniRec-0.1B in efficient and unified recognition.

Our main contributions are summarized as follows:

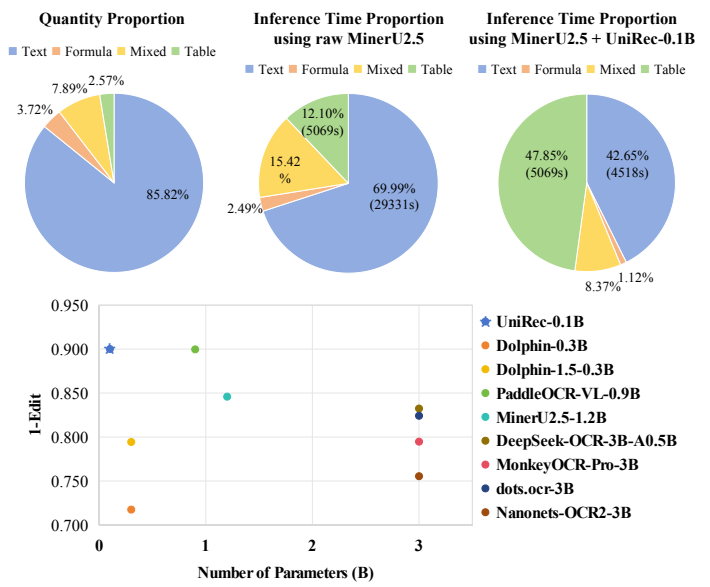


Figure 1 **Top:** Text and formulas take up 97.43% of page regions in quantity in OmniDocBench [44] (the first chart) and consume 87.90% of inference time in one A800 40G GPU by using raw MinerU2.5 [42] (the second chart). When replacing the corresponding MinerU2.5 modules by UniRec-0.1B, the parsing speed becomes 4× faster (the third chart). **Bottom:** Comparison with advanced document parsing models in our constructed UniRec-Bench. UniRec-0.1B outperforms or on par with existing models in accuracy while only has 3%-33% of their parameters.

- We construct UniRec40M containing 40 million multi-level text-formula samples in Chinese and English. It fills the data gap in unified text and formula recognition.
- We propose UniRec-0.1B, a lightweight unified recognition model. It addresses the granularity- and modality-mixed challenges by introducing Hierarchical Supervision Training and Semantics-Decoupled Tokenizer.
- Extensive evaluations show that UniRec-0.1B outperforms or is on par with leading large-scale VLM-based models in accuracy across various text and formula recognition tasks, while delivering a 2-9× inference speedup.

2 Related Work

2.1 Text and Formula Recognition

Text and formula recognition are traditionally treated as distinct tasks and both mainly focus on line-level recognition, aiming to convert text instances or mathematical formulas into symbolic or character sequences. In text recognition, existing methods are typically categorized into Connectionist Temporal Classification (CTC)-based methods [12, 16, 23, 27, 48] and encoder-decoder-based methods [3, 13, 18, 24, 29, 38, 47, 49, 60, 61, 68, 69, 73–77]. While CTC-based models emphasize fast inference, encoder-decoder-based ones generally have higher accuracy with increased computational cost. Most formula recognition (or mathematical expression recognition, MER) methods utilize the encoder-decoder framework [11, 37, 58, 64, 70, 71]. Adversarial and structure-aware models [64, 71], and Transformer or VLMs [37, 58] have significantly advanced this field. These approaches progressively improve syntactic parsing and contextual understanding of formulas. Despite these advancements, both text and formula recognition remain largely constrained to word- or line-level inputs, with paragraph- or multi-line recognition still relying on additional text and formula detection models.

2.2 Document Parsing with VLMs

With the rise of VLMs [2, 8, 22, 25, 54, 65, 66, 78], document parsing is increasingly moving toward unified models [4, 6, 7, 9, 28, 30, 34, 39, 41, 46, 62, 63]. Pioneering efforts such as Nougat [4] and GOT [62] introduce end-to-end frameworks that jointly recognize and extract multiple document elements, including text, formulas, tables, and charts, within a single model. These approaches demonstrate the feasibility of replacing traditional Optical Character Recognition (OCR) pipelines [10, 52, 59] with unified VLM-based solutions. Building on this paradigm, recent methods such as Ocean-OCR [7], olmOCR [46], dots.ocr [30], DeepSeek-OCR [63], and HunyuanOCR [53] employ multi-modal large language models [2, 32, 55] trained on extensive in-house document corpora to enhance end-to-end document parsing performance. While these unified models simplify system design and improve holistic reasoning, they often require large model sizes and incur substantial computational cost. An alternative line of work adopts multi-stage or hybrid designs that decouple layout analysis from content recognition, aiming to balance efficiency and recognition accuracy [9, 20, 31, 42]. Dolphin [20] utilizes a Swin-Transformer-based VLM for page-level layout parsing followed by parallel region recognition. MinerU2.5 [42] adopts a similar two-stage framework with a single vision-language model. MonkeyOCR [31] and PaddleOCR-VL [9] also follow a multi-stage strategy, integrating expert models for layout and reading-order analysis while employing VLMs for unified recognition of text, formulas, and tables. Although these methods unify multiple recognition tasks to reduce dependency on specialized models, they often increase parameter counts and reduce efficiency. In contrast, UniRec-0.1B focuses on lightweight unification of text and formula recognition, the two most dominant elements in documents. It maintains competitive accuracy while significantly improves parsing speed.

3 UniRec40M Dataset

3.1 Data Composition

As shown in Fig. 2, UniRec40M is built from three data sources to ensure diversity across domains and modality.

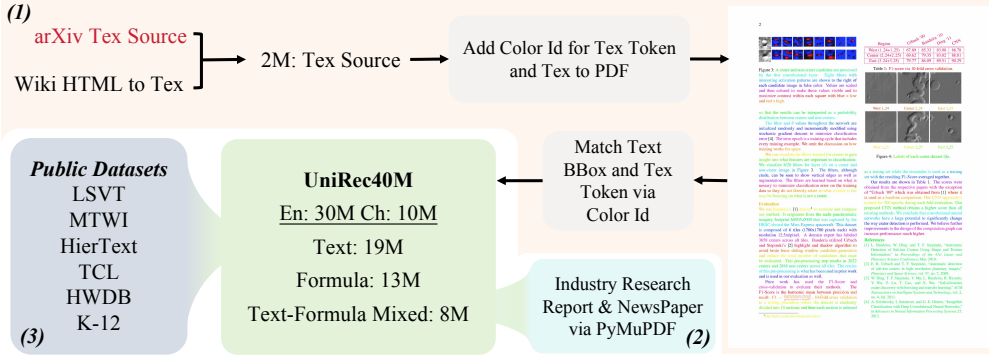


Figure 2 The construction and composition of UniRec40M. Detailed descriptions are provided in Sec. 3.

En-Text	TeX Generated						Scene Text			Handwritten			Domain Data			Sum
	En-Formula	En-Mixed	Ch-Text	Ch-Formula	Ch-Mixed	LSVT	MTWI	HierText	HWDB	TAL	Note	IR Report	Newspaper	K-12		
9.05	12.85	7.91	6.84	0.05	0.24	0.26	0.15	1.05	0.38	0.02	0.08	0.35	0.13	0.25	39.60	
1.68	2.57	0.64	1.86	0.05	0.24	1.30	1.03	0.32	1.13	0.20	0.41	0.70	0.25	0.25	12.63	

Table 1 Data composition of UniRec40M (per million). The last row presents the sampling counts of each epoch during training.

lities.

(1) Online TeX source [17]: We first collect arXiv¹ TeX source files and Wikipedia² HTML pages, which are also converted into TeX format. This results in approximately 2 million TeX files. For each TeX source, every valid text or formula token is assigned with a unique color by inserting the corresponding LaTeX color commands. The TeX files are then rendered into PDFs, producing documents with distinct colors for different textual and formulaic content. By performing color-based alignment between the TeX sources and the rendered PDFs, we can get labels at word and line levels, while the paragraph level can be obtained by further parsing LaTeX grammars. This pipeline enables the automatic generation of large-scale, multi-level data covering text, formula, and mixed text-formula content.

(2) Digital-born PDF documents: To broaden the distribution of document types, we collect digital-born PDFs such as industry research (IR) reports and newspapers. Then, we extract samples consisting of textual blocks and their corresponding image regions by PyMuPDF³. This component primarily supplements the dataset with multi-level, multi-domain text recognition data.

(3) Public datasets: We further integrate a range of public datasets to enhance coverage across languages and domains. It includes: Chinese scene text datasets: LSVT [50], MTWI [26]. English scene text dataset: HierText [35]. Handwritten datasets: CASIA-HWDB [33], TAL [51]. Examination-style dataset: K-12 [51]. Additionally, we include handwritten notes (Note) labeled with Qwen3VL-235B-A30B [65] and manually refined, serving as high-quality handwritten supplements.

Tab. 1 summarizes the composition of UniRec40M, which has nearly 30M English and 10M Chinese samples. Specifically, the dataset includes 19M plain text, 13M formula-only, and 8M text-formula mixed instances. This large-scale, multilingual collection provides rich annotations for a broad coverage of real-world document formats, thus can serve as the foundation for training UniRec-0.1B.

3.2 Sampling Strategy

To ensure balanced learning across data modalities, we adopt a proportion-balanced sampling strategy. Each

¹<https://www.arxiv.org/>

²<https://www.wikipedia.org/>

³<https://pymupdf.readthedocs.io/>

data type is either sub-sampled or re-sampled per training epoch, maintaining stable ratios among text, formula, and mixed samples. The last row of Tab. 1 reports the sampling counts used in each epoch during training.

4 UniRec-0.1B Model

The architecture of UniRec-0.1B follows a standard encoder-decoder framework, as illustrated in Fig. 3. The image encoder, and the input image follows a native resolution strategy, where the input image maintains its original aspect ratio, with the maximum width and height capped at 960 and 1408 pixels, respectively.

Formally, the input image is defined as $\mathbf{I} \in \mathbb{R}^{H \times W \times 3}$. The image encoder $\text{Encoder}(\cdot)$ is implemented with FocalNet [67], producing a dense visual feature map:

$$\mathbf{F}_{map} = \text{Encoder}(\mathbf{I}) \in \mathbb{R}^{\frac{H}{32} \times \frac{W}{32} \times D}$$

where $D = 768$ denotes the feature dimensionality.

To obtain a sequence representation, the spatial dimensions of \mathbf{F}_{map} are flattened into a set of visual tokens:

$$\mathbf{F} = \text{Flatten}(\mathbf{F}_{map}) \in \mathbb{R}^{N \times D}, \quad N = \frac{H}{32} \times \frac{W}{32}.$$

This tokenized feature sequence serves as the input to the subsequent multimodal decoder. The text and formula supervision Label is defined with hierarchical supervision tokens. A Semantic-Decoupled Tokenizer (SDT) is employed to decouple textual and formulaic elements, yielding a discrete token sequence:

$$\mathbf{Y} = \text{SDT}(\text{Label}) = \{\text{<BOS>} , y_0, y_1, \dots, y_{l-1}, \text{<EOS>}\},$$

where <BOS> and $y_l = \text{<EOS>}$ represent the beginning and end of sequence, respectively, and l denotes the token length. Each token is mapped to a continuous embedding via a text embedding layer $\mathbf{T} = \mathbf{E}_{text}(\mathbf{Y}) \in \mathbb{R}^{(l+2) \times D}$, where the embedding matrix is defined as $\mathbf{E}_{text} \in \mathbb{R}^{|V| \times D}$ and $|V|$ is the vocabulary size.

The decoder $\text{Decoder}(\cdot)$ consists of six Transformer layers with cross-attention modules. Each layer operates with hidden size D and $D/64$ attention heads. Given the textual embeddings \mathbf{T} and the visual features \mathbf{F} , the decoder performs autoregressive generation under a causal mask \mathbf{M}_{causal} :

$$\tilde{\mathbf{Y}} = \text{Decoder}(\mathbf{T}, \mathbf{F}, \mathbf{M}_{causal}) = \{\tilde{y}_0, \tilde{y}_1, \dots, \tilde{y}_l\}.$$

At each time step t , the model predicts the next token probability $P(\tilde{y}_t | \tilde{y}_{0:t-1}, \mathbf{F}) = \text{Softmax}(h_t W_o)$, where h_t is the decoder hidden state and $W_o \in \mathbb{R}^{D \times |V|}$ is the output projection matrix. The model is trained with a cross-entropy loss over all token positions:

$$\mathcal{L}_{CE} = - \sum_{t=0}^l \log P(y_t | y_{0:t-1}, \mathbf{F}).$$

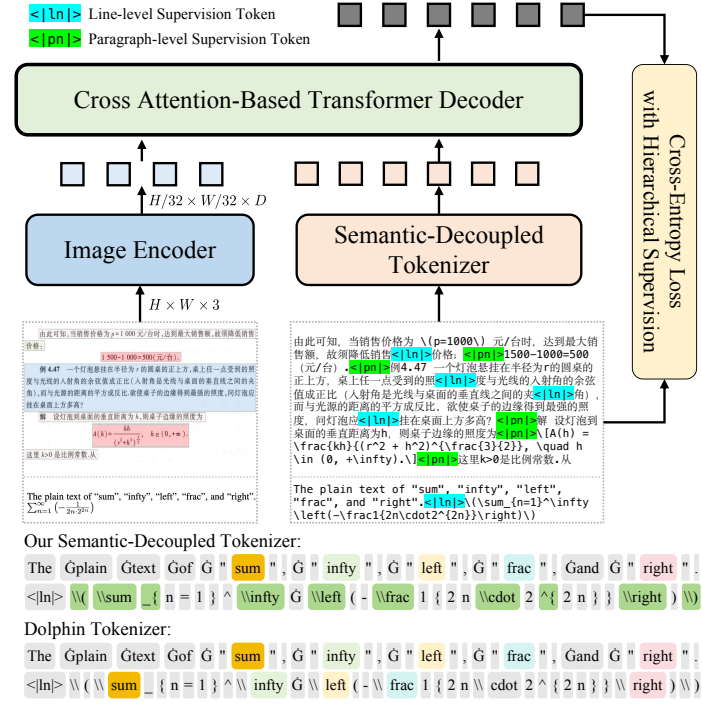


Figure 3 The architecture overview of UniRec-0.1B. ‘G’ represents a space. Detailed descriptions are provided in Sec. 4.

4.1 Hierarchical Supervision Training

Text and formula exhibit a natural hierarchical structure, typically organized into lines and paragraphs. Most recognition models treat the content as a flat sequence, ignoring the hierarchical spatial relationships between lines and paragraphs. This simplification limits the model’s ability to learn the spatial layout representation.

To explicitly model this hierarchy, we introduce line-level and paragraph-level supervision tokens, $\langle | 1n | \rangle$ and $\langle | pn | \rangle$, during dataset construction, as shown in Fig. 3. The token $\langle | 1n | \rangle$ denotes a line break within a paragraph, while $\langle | pn | \rangle$ indicates the end of a paragraph. These supervision signals encourage the model to learn hierarchical spatial dependencies and improve layout awareness during training. During inference, predicted $\langle | 1n | \rangle$ tokens are removed, and $\langle | pn | \rangle$ tokens are replaced with two newline characters to reconstruct the paragraph structure in the generated output.

4.2 Semantic-Decoupled Tokenizer

Existing tokenizers are usually trained on a joint corpus that mixes plain text and formula. This approach often leads to semantic coupling between textual and formula tokens. For example, in the Dolphin Tokenizer (see Fig. 3), tokens such as *sum*, *infty*, *left*, *frac*, and *right* are assigned shared embeddings despite representing semantically distinct concepts in plain text and formula modalities. While LLMs can leverage contextual cues to disambiguate such cases, this coupling introduces unnecessary learning complexity for smaller models like UniRec-0.1B.

To mitigate this issue, we propose a semantic-decoupled tokenizer. Specifically, we train two independent tokenizers: one on plain text and another on mathematical formulas. The tokens from the formula tokenizer are then integrated into the text tokenizer as special tokens, excluding those already present in the text ones. As shown in Fig. 3, this method ensures that tokens such as *sum*, *infty*, *left*, *frac*, and *right* maintain distinct embeddings across modalities, thereby achieving effective semantic decoupling and reducing representational ambiguity during model training.

5 Experiments

5.1 Benchmark and Implementation Details

UniRec-Bench: Recent document parsing benchmarks, such as FoxPage [62], olmOCR-Bench [46], and OmniDocBench [44], primarily focus on evaluating page-level parsing capabilities. They lack fine-grained evaluation at the granularity of text block. To bridge this gap, we extend OmniDocBench [44] by extracting text, formula, and mixed text-formula blocks from full-page documents. Then, each text block is further categorized into five hierarchical levels and two languages. Consistent with OmniDocBench, the dataset spans nine document domains. This process yields UniRec-Bench (see Tab. 2 and Tab. 3), a comprehensive benchmark that emphasizes multi-type, level, lingual, and domain text block evaluation. Benefiting from its fine-grained categorization, UniRec-Bench can support the inspection of different parsing models at the block level, which is largely missed in existing studies.

Training: We use AdamW optimizer [36] with a weight decay of 0.01 for training. The learning rate (LR) is set to 1×10^{-4} and the global batchsize is set to 64. One cycle LR scheduler [57] with 0.5 epochs linear warm-up is used in all the 10 epochs. Data augmentation like rotation, distortion, motion blur and gaussian noise, are randomly performed. The maximum token length is set to 1024. The vocabulary size $|V|$ is 56371. Training takes approximately 80 hours on 8 A800 40GB GPUs. Note that UniRec-0.1B is trained from scratch without loading pre-trained models. The accuracy is computed based on the edit distance between the model prediction and the ground-truth.

5.2 Ablation Study

We carry out ablation studies to assess the effectiveness of the proposed HST and SDT on UniRec-0.1B. The results are summarized in Tab. 2 and Tab. 3.

Methods	Size	Avg	Modality			Character	Word	Line	Level			Language			
			Text	Formula	Mix				167	2525	3549	7334	Multi-Paragraph	726	CH
PP-OCRv5 [10]	42M	-	0.125	-	-	0.597	0.208	0.100	0.097	-	-	0.138	0.097	0.197	0.109
PP-Recv5 [10]	20M	-	-	-	-	0.033	0.056	0.094	-	-	-	-	-	-	-
OpenOCR-Rec [16]	30M	-	-	-	-	0.054	0.061	0.079	-	-	-	-	-	-	-
Mathpix [40]	-	-	-	0.322	-	-	-	-	-	-	-	-	-	-	-
Pix2Tex [37]	23M	-	-	0.337	-	-	-	-	-	-	-	-	-	-	-
UniMERNNet-B [58]	0.3B	-	-	0.238	-	-	-	-	-	-	-	-	-	-	-
Dolphin [20]	0.3B	0.283	0.118	0.502	0.227	0.072	0.070	0.065	0.153	-	-	0.204	0.141	0.047	0.183
Dolphin-1.5 [20]	0.3B	0.206	0.050	0.365	0.202	0.061	0.059	0.056	0.037	-	-	0.115	0.049	0.038	0.110
MonkeyOCR-Pro [31]	3B	0.205	0.297	0.177	0.142	0.043	0.055	0.111	0.490	-	-	0.157	0.408	0.065	0.147
dots.ocr [30]	3B	0.176	0.113	0.221	0.194	0.129	0.148	0.192	0.065	-	-	0.092	0.121	0.096	0.107
MinerU2.5 [42]	1.2B	0.154	0.167	0.140	0.155	0.033	0.051	0.068	0.260	-	-	0.153	0.217	0.055	0.138
Nanonets-OCR2 [39]	3B	0.245	0.312	0.193	0.229	0.174	0.077	0.099	0.504	-	-	0.263	0.392	0.139	0.221
DeepSeek-OCR [63]	3B-A0.5B	0.168	0.103	0.238	0.162	0.794	0.219	0.061	0.067	-	-	0.107	0.103	0.106	0.091
PaddleOCR-VL [9]	0.9B	0.100	0.041	0.125	0.135	0.037	0.042	0.046	0.031	-	-	0.107	0.044	0.022	0.087
UniRec-0.1B	0.1B	0.100	0.038	0.134	0.128	0.025	0.032	0.043	0.032	-	-	0.099	0.041	0.023	0.071
w/o HST w SDT	0.1B	0.113	0.050	0.144	0.143	0.030	0.040	0.047	0.049	-	-	0.111	0.053	0.034	0.083
w/o HST w/o SDT	0.1B	0.159	0.062	0.255	0.161	0.054	0.066	0.066	0.053	-	-	0.114	0.070	0.035	0.092

Table 2 Comparison with text recognition expert models, formula recognition expert models, and document parsing expert models on UniRec-Bench across modalities, levels, and languages. The last two rows present ablation experiments for UniRec-0.1B.

Methods	Size	Book	Domain								
			970	PPT2PDF	Research Report	Textbook	Exam Paper	Magazine	Literature	Note	Newspaper
PP-OCRv5 [10]	42M	0.100	0.101	-	0.051	0.114	0.155	0.081	0.088	0.250	0.132
Dolphin [20]	0.3B	0.033	0.060	-	0.040	0.069	0.119	0.043	0.021	0.238	0.167
Dolphin-1.5 [20]	0.3B	0.024	0.045	-	0.027	0.039	0.075	0.029	0.020	0.184	0.045
MonkeyOCR-Pro [31]	3B	0.025	0.075	-	0.030	0.044	0.082	0.023	0.010	0.200	0.585
dots.ocr [30]	3B	0.027	0.064	-	0.034	0.056	0.085	0.028	0.021	0.126	0.184
MinerU2.5 [42]	1.2B	0.024	0.107	-	0.031	0.044	0.086	0.019	0.015	0.151	0.302
Nanonets-OCR2 [39]	3B	0.067	0.124	-	0.051	0.097	0.133	0.061	0.092	0.265	0.556
DeepSeek-OCR [63]	3B-A0.5B	0.071	0.136	-	0.053	0.111	0.137	0.061	0.037	0.224	0.105
PaddleOCR-VL [9]	0.9B	0.021	0.060	-	0.023	0.042	0.085	0.019	0.013	0.067	0.039
UniRec-0.1B	0.1B	0.025	0.063	-	0.018	0.054	0.058	0.021	0.012	0.055	0.038
w/o HST w SDT	0.1B	0.026	0.091	-	0.024	0.071	0.087	0.026	0.015	0.073	0.050
w/o HST w/o SDT	0.1B	0.025	0.120	-	0.030	0.065	0.090	0.033	0.019	0.075	0.071

Table 3 Comparison with existing models and ablations across domains on UniRec-Bench.

Effectiveness of HST. The last second row in Tab. 2 and Tab. 3 reports the performance without HST. Incorporating HST improves the edit distance by 1.2% on text, 1.0% on formulas, and 1.5% on their mix, indicating consistent benefits across all scenarios. For multi-level text, the five levels get 0.5%, 0.8%, 0.4%, 1.7%, and 1.2% improvements, respectively. Gains are particularly notable at the paragraph and multi-paragraph levels, demonstrating that hierarchical supervision effectively captures structural dependencies across lines and paragraphs. Meanwhile, benefits are also observed across languages. For multiple document domains, the most pronounced improvements are observed on *PPT2PDF* and *Exam Paper* subsets, with increases of 2.8% and 2.9%, respectively. This is mainly because PPT and exam documents often have complex layouts compared to other domains, and HST better models such structural complexity, leading to enhanced recognition.

Effectiveness of SDT. The last row in Tab. 2 and Tab. 3 shows the results further without SDT. Using SDT yields 1.2% improvement on text, 11.1% on formulas, and 1.8% on their mix. The results confirm the benefit of SDT. Specifically, the substantial gain in formula recognition convincingly suggests that decoupling formula and text tokens alleviates semantic entanglement between modalities. In addition, SDT slightly decreases performance in certain domains, such as *Textbook*, with a 0.6% drop. Nevertheless, when SDT is combined with HST, all domains benefit, leading to an average gain of 2.4%.

Method Type	Methods	Overall ^{Edit} ↓	Overall ^{Edit} ↓		Text ^{Edit} ↓		Formula ^{Edit} ↓		Table ^{TEDS} ↑		Table ^{Edit} ↓		Reading Order ^{Edit} ↓	
			EN	CH	EN	CH	EN	CH	EN	CH	EN	CH	EN	CH
Pipeline Models	Doclinc-2.14.0 [52]	0.749	0.589	0.909	0.416	0.987	0.999	1	61.3	25.0	0.627	0.810	0.313	0.837
	OpenParse-0.7.0 [21]	0.730	0.646	0.814	0.681	0.974	0.996	1	64.8	27.5	0.284	0.639	0.595	0.641
	Unstructured-0.17.2 [56]	0.651	0.586	0.716	0.198	0.481	0.999	1	0	0.1	1	0.998	0.145	0.387
	Pix2Text-1.1.2.3 [5]	0.424	0.320	0.528	0.138	0.356	0.276	0.611	73.6	66.2	0.584	0.645	0.281	0.499
	Marker-1.7.1 [45]	0.397	0.296	0.497	0.085	0.293	0.374	0.688	67.6	54.0	0.609	0.678	0.116	0.329
	Mathpix [40]	0.278	0.191	0.364	0.105	0.381	0.306	0.454	77.0	67.1	0.243	0.320	0.108	0.304
	MinerU-pipeline [59]	0.203	0.162	0.244	0.072	0.111	0.313	0.581	77.4	79.5	0.166	0.150	0.097	0.136
General VLMs	PP-StructureV3 [10]	0.176	0.145	0.206	0.058	0.088	0.295	0.535	77.2	83.9	0.159	0.109	0.069	0.091
	InternVL2-76B [8]	0.442	0.440	0.443	0.353	0.290	0.543	0.701	63.0	60.2	0.547	0.555	0.317	0.228
	GPT-4o [1]	0.316	0.233	0.399	0.144	0.409	0.425	0.606	72.0	62.9	0.234	0.329	0.128	0.251
	InternVL3-78B [78]	0.257	0.218	0.296	0.117	0.210	0.380	0.533	69.0	73.9	0.279	0.282	0.095	0.161
	Qwen2.5-VL-72B [2]	0.238	0.214	0.261	0.092	0.180	0.315	0.434	81.4	83.0	0.341	0.262	0.106	0.168
	Gemini2.5-Pro [22]	0.180	0.148	0.212	0.055	0.168	0.356	0.439	85.8	86.4	0.130	0.119	0.049	0.121
Specialized VLMs	Nougat [4]	0.713	0.452	0.973	0.365	0.998	0.488	0.941	39.9	0.0	0.572	1	0.382	0.954
	SmolDocling-256M [41]	0.655	0.493	0.816	0.262	0.838	0.753	0.997	44.9	16.5	0.729	0.907	0.227	0.522
	olmOCR-7B [46]	0.398	0.326	0.469	0.097	0.293	0.455	0.655	68.1	61.3	0.608	0.652	0.145	0.277
	GOT [62]	0.349	0.287	0.411	0.189	0.315	0.360	0.528	53.2	47.2	0.459	0.520	0.141	0.280
	OCRFlux-3B [6]	0.294	0.238	0.349	0.112	0.256	0.447	0.716	69.0	80.0	0.269	0.162	0.126	0.263
	Nanonets-OCR-s [39]	0.289	0.283	0.295	0.134	0.231	0.518	0.546	76.8	79.4	0.343	0.201	0.135	0.200
	Dolphin [20]	0.259	0.205	0.313	0.092	0.204	0.447	0.606	76.1	66.9	0.193	0.282	0.088	0.160
	MinerU2-VLM [43]	0.186	0.133	0.238	0.045	0.115	0.273	0.506	82.1	83.4	0.150	0.209	0.066	0.122
	MonkeyOCR-1.2B [31]	0.184	0.146	0.221	0.068	0.118	0.272	0.452	81.3	85.5	0.149	0.134	0.093	0.179
	MonkeyOCR-3B [31]	0.172	0.138	0.206	0.067	0.107	0.246	0.421	81.5	87.5	0.139	0.111	0.100	0.185
UniRec-0.1B	dots.ocr [30]	0.143	0.125	0.160	0.032	0.066	0.329	0.416	88.6	89.0	0.099	0.092	0.040	0.067
	DeepSeek-OCR [63]	0.158	0.134	0.181	0.046	0.097	0.285	0.433	82.6	89.0	0.138	0.088	0.067	0.105
	olmOCR2 [46]	0.214	0.161	0.267	0.048	0.185	0.392	0.543	83.7	78.5	0.123	0.165	0.081	0.174
	MinerU2.5 [42]	0.143	0.111	0.174	0.050	0.074	0.258	0.473	88.3	89.2	0.089	0.083	0.045	0.068
PaddleOCR-VL	w UniRec-0.1B	0.120	0.107	0.133	0.044	0.068	0.247	0.314	88.3	89.2	0.089	0.083	0.047	0.067
	PaddleOCR-VL [9]	0.115	0.105	0.126	0.041	0.062	0.241	0.316	88.0	92.1	0.093	0.062	0.045	0.063
	w UniRec-0.1B	0.113	0.102	0.123	0.040	0.065	0.234	0.298	88.0	92.1	0.093	0.062	0.042	0.065

Table 4 Evaluation of document parsing on OmniDocBench [44]. *w* UniRec-0.1B means replacing the text and formula recognition modules of MinerU2.5 [42] or PaddleOCR-VL [9] by UniRec-0.1B, while keep their layout analysis and table recognition remain unchanged.

5.3 Comparison with State-of-the-arts

We compare UniRec-0.1B with state-of-the-art text recognition expert models, formula recognition expert models, document parsing models, and general VLMs on UniRec-Bench and OmniDocBench [44]. UniRec-Bench focuses on text and formula block recognition, while OmniDocBench [44] targets full-page parsing.

5.3.1 Results on UniRec-Bench

Comparison with text recognition expert models. For text recognition, we benchmark against advanced open-source models, including PP-OCRv5 [10], PP-Recv5 [10], and OpenOCR-Rec [16]. PP-OCRv5 combines a text-line detector (PP-Detv5) and a recognizer (PP-Recv5) to perform paragraph-level text recognition. Since PP-Recv5 and OpenOCR-Rec operate only text instances rather than paragraphs, they are evaluated at the character-, word-, and line-levels. Although the two small expert models are known for their strong performance in line-level recognition, results in Tab. 2 show that UniRec-0.1B consistently outperforms them across multiple text levels in Chinese, English, and mixed-language text. In addition, UniRec-0.1B largely surpasses the pipeline-based PP-OCRv5 across all domains, as shown in Tab. 3. These results indicate that unified multi-level text recognition not only eliminates the need for a separate text detection module but also improves the overall accuracy, validating the effectiveness of UniRec-0.1B.

Comparison with formula recognition expert models. For formula recognition, we compare ours with commercial Mathpix [40], open-source Pix2Tex [37] and UniMERNNet-B [58]. As reported in Tab. 2, UniRec-0.1B outperforms them by 18.8%, 20.3%, and 10.4%, respectively. The performance gain mainly stems from the rich and diverse formula recognition data in UniRec40M that leads to sufficient model training, and the

Methods	Size	Character	Word	Line	Paragraph	Multi-Paragraph	Block _{avg}	Page _{avg}
MonkeyOCR [31]	3B	0.64	0.76	1.25	4.43	5.60	3.62	58.39
DeepSeek-OCR [63]	3B-A0.5B	0.18	0.94	0.93	4.33	6.92	3.47	58.95
MinerU2.5 [42]	1.2B	0.08	0.24	0.66	3.16	7.92	2.54	42.72
PaddleOCR-VL [9]	0.9B	0.60	0.66	0.9	2.29	3.32	1.88	31.92
Dolphin-1.5 [20]	0.3B	0.10	0.14	0.34	0.95	1.14	0.78	13.16
UniRec-0.1B	0.1B	0.03	0.05	0.10	0.54	0.62	0.37	6.20

Table 5 Inference speed (in second) comparison across models. The speed is measured on a single A800 40GB GPU. For fairness, all models are run without inference acceleration, using Torch or PaddlePaddle in dynamic graph mode with KV Cache and a batch size of 1.

说	R	4	甲	1. 沧海桑田 70	10	Finding	中邮证券对于本申明具有最终解释权。	
Label: 说	R	4	甲	1. 沧海桑田 70	10	Finding	中邮证券对于本申明具有最终解释权。	
Dolphin-1.5: 说	R	4	甲	1. 沧海桑田 70	10	Finding	中邮证券对于本申明具有最终解释权。	
PaddleOCR-VL: 说	R	4	甲	1. 沧海桑田 70	10	Finding	中邮证券对于本申明具有最终解释权。	
MinerU2.5: 说	R	4	甲	1. 沧海桑田 70	10	Finding	中邮证券对于本申明具有最终解释权。	
MonkeyOCR: 说	R	4	甲	1. 沧海桑田 70	10	Finding	中邮证券对于本申明具有最终解释权。	
dots.ocr: 说	R	4	甲	1. 沧海桑田 70	10	Fiunding	中邮证券对于本申明具有最终解释权。	
Nanonets-OCR2: 说	R	$\$\\mathbf{4}$	甲	1. 沧海桑田 70	10	Finding	中邮证券对于本申明具有最终解释权。	
DeepSeek-OCR: *	*	4	面	1. 泡菜退市 \[T_0 \]	TC	Friendings	中邮证券对于本申明具有最终解释权。	
UniRec-0.1B: 说	R	4	甲	1. 沧海桑田 70	10	Finding	中邮证券对于本申明具有最终解释权。	
MnO ₂								
2. (1) 锥形瓶 (2) 2H ₂ O ₂ $\xrightarrow{\text{浓硫酸}}$ 2H ₂ O + O ₂ ↑ E 浓硫酸								
Label: 2.	(1)	锥形瓶	(2)	$2H_2O_2 \xrightarrow{\text{浓硫酸}}$	2H ₂ O + O ₂ ↑ E 浓硫酸	Dated: January 30, 2019.	Dated: January 30, 2019.	
Dolphin-1.5:	2.	(1)	锥形瓶	(2)	$2H_2O_2 \xrightarrow{\text{浓硫酸}}$	Dated: January 30, 2019.	Dated: January 30, 2019.	
PaddleOCR-VL:	2.	(1)	锥形瓶	(2)	$2H_2O_2 \xrightarrow{\text{浓硫酸}}$	Dated: January 30, 2019.	Dated: January 30, 2019.	
MinerU2.5:	MnO ₂	2H2O ₂	E	浓硫酸	Dated: January 30, 2019.	Dated: January 30, 2019.		
MonkeyOCR:	2.	(1)	锥形瓶	(2)	$2H_2O_2 \xrightarrow{\text{浓硫酸}}$	Dated: January 30, 2019.	Dated: January 30, 2019.	
dots.ocr:	2.	(1)	锥形瓶	(2)	$2H_2O_2 \xrightarrow{\text{浓硫酸}}$	Dated: January 30, 2019.	Dated: January 30, 2019.	
Nanonets-OCR2:	2.	(1)	锥形瓶	(2)	$2H_2O_2 \xrightarrow{\text{浓硫酸}}$	Dated: January 30, 2019.	Dated: January 30, 2019.	
DeepSeek-OCR:	2.	(1)	锥形瓶	(2)	$2H_2O_2 \xrightarrow{\text{浓硫酸}}$	Dated: January 30, 2019.	Dated: January 30, 2019.	
UniRec-0.1B:	2.	(1)	锥形瓶	(2)	$2H_2O_2 \xrightarrow{\text{浓硫酸}}$	Dated: January 30, 2019.	Dated: January 30, 2019.	

Figure 4 Recognition result visualizations. Red characters indicate recognition errors, indicate missed characters, and * indicate recognition results that are meaningless hallucination. Green indicates correct recognition. More cases are presented in the supplementary.

decoupled tokenizer design that well separates textual and formula semantics.

Comparison with document parsing models. UniRec-0.1B also exhibits clear advantages when compared with VLM-based document parsing models. Against Dolphin-1.5 [20], a model with 0.3B parameters, UniRec-0.1B achieves improvements of 1.2% on text, 23.1% on formulas, and 7.4% on their mix. The substantial gain in formula recognition is largely attributed to UniRec-0.1B’s text-formula SDT design, whereas Dolphin-1.5 uses a semantically coupled tokenizer, making it difficult to distinguish text from formula elements at small parameter scales. Moreover, as reported in Tab. 5, UniRec-0.1B is more than 2× faster than Dolphin-1.5. Compared to PaddleOCR-VL [9], UniRec-0.1B achieves comparable performance using only 11% of its parameters, consistently across multiple levels, languages, and domains. Notably, in the *Exam Paper* domain, UniRec-0.1B outperforms PaddleOCR-VL by 2.7%. This prominent gain is likely due to the inclusion of exam-related samples in UniRec40M, highlighting the importance of incorporating multi-domain data during dataset construction. Regarding inference speed, compared to PaddleOCR-VL, UniRec-0.1B reduces the inference time from 1.88 s to 0.37 s on the block level, and from 31.92 s to 6.2 s on the page level, both exceeding 5× speedup.

Furthermore, UniRec-Bench reveals that end-to-end full-page parsing models such as dots.ocr [30], Nanonets-OCR2 [39], and DeepSeek-OCR [63] perform worse at the character, word, and line levels. The first eight cases in Fig. 4 also confirm this observation. In contrast, multi-stage methods such as Dolphin [20], MonkeyOCR [31], MinerU2.5 [42], and PaddleOCR-VL [9] excel in fine-grained character-, word-, and line-level recognition. End-to-end methods more emphasize holistic perception, while multi-stage methods integrate multiple expert models that are good at specialized fine-grained recognition. Nevertheless, our UniRec-0.1B absorbs advantages from both sides. It not only achieves SOTA accuracy in character, word, and line levels, but also

attains highly competitive accuracy in paragraph and multi-paragraph levels. These results again validate the effectiveness of UniRec-0.1B.

Note that in *Note* domain, UniRec-0.1B gets the best accuracy, surpassing PaddleOCR-VL by 1.2%, while other models lag significantly behind. This suggests that most methods are optimized for machine-written documents but struggle with handwritten ones. Similarly, in *Newspaper* domain, UniRec-0.1B again achieves the best result, with PaddleOCR-VL and Dolphin-1.5 performing nearby, and the rest fall far behind. This is explained as *Newspaper* pages often contain blurred or degraded text. The results indicate that most existing methods are biased toward digital-born documents and tend to fail on visually noisy inputs.

5.3.2 Results on OmniDocBench

To evaluate the document parsing performance of UniRec-0.1B, we conduct experiments summarized in Tab. 4. Specifically, we integrate UniRec-0.1B into two leading two-stage document parsing methods, MinerU2.5 and PaddleOCR-VL, by replacing their text and formula recognition modules with UniRec-0.1B. The two methods perform layout analysis in the first stage, followed by region-level recognition in the second stage, where detected document components (e.g., text or formula regions) are cropped and recognized individually. In our setup, the second-stage recognition of text and formula regions is implemented by UniRec-0.1B.

As shown in Tab. 4, when combined with MinerU2.5, the full-page edit distance improves from 0.143 to 0.120, achieving a 2.3% performance gain. Moreover, as reported in Tab. 5, UniRec-0.1B reduces the average page parsing time from 42.72 s to 6.2 s, resulting in a nearly 7 \times speedup. A similar trend is observed with PaddleOCR-VL, where the full-page edit distance improves further by 0.2%, reaching the new SOTA, and the parsing time accelerated significantly. These results clearly demonstrate the practicality and effectiveness of UniRec-0.1B in document parsing systems. Moreover, they also verify the necessity and benefit of unified recognition of both text and formulas with a lightweight model.

6 Conclusion

In this paper, we have presented UniRec-0.1B, a 0.1B lightweight model that is capable of jointly recognize text and formulas across multiple hierarchical levels effective and efficient. To build this model, we first construct UniRec40M, a comprehensively labeled dataset comprising 40 million text, formula, and their mix samples in both Chinese and English. It fills the data gap in unified text-formula recognition. Furthermore, we have made two key innovations to unleash the recognition capability of the model: Hierarchical Supervision Training and Semantics-Decoupled Tokenizer. The former explicitly models the hierarchical relationships between lines and paragraphs, while the latter decouples token representations for text and formulas. UniRec-0.1B, the resulted model, has been extensively validated on the popular OmniDocBench and the newly constructed UniRec-Bench, which evaluates text and formula blocks of multiple levels, languages, and domains. The results demonstrate that UniRec-0.1B achieves leading accuracy compared to existing models, meanwhile it achieves 2-9 \times speedup in inference speed. This clearly validates its effectiveness, and the practicality that we use a lightweight model for unified text and formula recognition. Furthermore, the results on UniRec-Bench reveals some limitations of existing models, e.g., excelling at paragraph-level recognition but struggling with fine-grained recognition. These constitute future research directions. Overall, we hope that our UniRec-0.1B, UniRec40M, and UniRec-Bench will continue to advance the field of document parsing.

References

- [1] Josh Achiam, Steven Adler, Sandhini Agarwal, Lama Ahmad, Ilge Akkaya, Florencia Leoni Aleman, Diogo Almeida, Janko Altenschmidt, Sam Altman, Shyamal Anadkat, et al. Gpt-4 technical report. [arXiv preprint arXiv:2303.08774](https://arxiv.org/abs/2303.08774), 2023.
- [2] Shuai Bai, Keqin Chen, Xuejing Liu, Jialin Wang, Wenbin Ge, Sibo Song, Kai Dang, Peng Wang, Shijie Wang, Jun Tang, et al. Qwen2. 5-vl technical report. [arXiv preprint arXiv:2502.13923](https://arxiv.org/abs/2502.13923), 2025.
- [3] Darwin Bautista and Rowel Atienza. Scene text recognition with permuted autoregressive sequence models. In [ECCV](https://openaccess.thecvf.com/content_ECCV_2022/html/Bautista_Scene_Text_Recognition_with_Permuted_Autoregressive_Sequence_Models_ECCV_2022_paper.html), pages 178–196. Springer, 2022.
- [4] Lukas Blecher, Guillem Cucurull, Thomas Scialom, and Robert Stojnic. Nougat: Neural optical understanding for academic documents. [arXiv preprint arXiv:2308.13418](https://arxiv.org/abs/2308.13418), 2023.
- [5] breezedeus. Pix2text. <https://github.com/breezedeus/Pix2Text>, 2022. Accessed: 2025-06-23.
- [6] chatdoc com. Ocrflux. <https://github.com/chatdoc-com/OCRFlux>, 2025. Accessed: 2025-09-25.
- [7] Song Chen, Xinyu Guo, Yadong Li, Tao Zhang, Mingan Lin, Dongdong Kuang, Youwei Zhang, Lingfeng Ming, Fengyu Zhang, Yuran Wang, et al. Ocean-ocr: Towards general ocr application via a vision-language model. [arXiv preprint arXiv:2501.15558](https://arxiv.org/abs/2501.15558), 2025.
- [8] Zhe Chen, Jiannan Wu, Wenhui Wang, Weijie Su, Guo Chen, Sen Xing, Muyan Zhong, Qinglong Zhang, Xizhou Zhu, Lewei Lu, et al. Internvl: Scaling up vision foundation models and aligning for generic visual-linguistic tasks. In [CVPR](https://openaccess.thecvf.com/content_CVPR_2024/html/Chen_Internvl_Scaling_up_Vision_Foundation_Models_and_Aligning_for_Generic_Visual-Linguistic_Tasks_CVPR_2024_paper.html), pages 24185–24198, 2024.
- [9] Cheng Cui, Ting Sun, Suyin Liang, Tingquan Gao, Zelun Zhang, Jiaxuan Liu, Xueqing Wang, Changda Zhou, Hongen Liu, Manhui Lin, et al. Paddleocr-vl: Boosting multilingual document parsing via a 0.9 b ultra-compact vision-language model. [arXiv preprint arXiv:2510.14528](https://arxiv.org/abs/2510.14528), 2025.
- [10] Cheng Cui, Ting Sun, Manhui Lin, Tingquan Gao, Yubo Zhang, Jiaxuan Liu, Xueqing Wang, Zelun Zhang, Changda Zhou, Hongen Liu, et al. Paddleocr 3.0 technical report. [arXiv preprint arXiv:2507.05595](https://arxiv.org/abs/2507.05595), 2025.
- [11] Yuntian Deng, Anssi Kanervisto, Jeffrey Ling, and Alexander M Rush. Image-to-markup generation with coarse-to-fine attention. In [ICML](https://openaccess.thecvf.com/content_ICML_2017/html/Deng_Image-to-Markup_Generation_With_Coarse-to-Fine_Attention_ICML_2017_paper.html), pages 980–989. PMLR, 2017.
- [12] Yongkun Du, Zhineng Chen, Caiyan Jia, Xiaoting Yin, Tianlun Zheng, Chenxia Li, Yuning Du, and Yu-Gang Jiang. SVTR: Scene text recognition with a single visual model. In [IJCAI](https://openaccess.thecvf.com/content_IJCAI_2022/html/Du_SVTR_Scene_Text_Recognition_With_A_Single_Visual_Model_IJCAI_2022_paper.html), pages 884–890, 2022.
- [13] Yongkun Du, Zhineng Chen, Caiyan Jia, Xieping Gao, and Yu-Gang Jiang. Out of length text recognition with sub-string matching. In [AAAI](https://openaccess.thecvf.com/content_AAAI_2025/html/Du_Out_of_Length_Text_Recognition_With_Sub-String_Matching_AAAI_2025_paper.html), pages 2798–2806, 2025.
- [14] Yongkun Du, Zhineng Chen, Caiyan Jia, Xiaoting Yin, Chenxia Li, Yuning Du, and Yu-Gang Jiang. Context perception parallel decoder for scene text recognition. [IEEE Trans. Pattern Anal. Mach. Intell.](https://ieeexplore.ieee.org/abstract/document/9545453), 47(6):4668–4683, 2025. doi: 10.1109/TPAMI.2025.3545453.
- [15] Yongkun Du, Zhineng Chen, Yuchen Su, Caiyan Jia, and Yu-Gang Jiang. Instruction-guided scene text recognition. [IEEE Trans. Pattern Anal. Mach. Intell.](https://ieeexplore.ieee.org/abstract/document/9525526), 47(4):2723–2738, 2025. doi: 10.1109/TPAMI.2025.3525526.
- [16] Yongkun Du, Zhineng Chen, Hongtao Xie, Caiyan Jia, and Yu-Gang Jiang. SVTRv2: Ctc beats encoder-decoder models in scene text recognition. In [ICCV](https://openaccess.thecvf.com/content_ICCV_2025/html/Du_SVTRv2_Ctc_beats_Encoder-Decoder_Models_in_Scene_Text_Recognition_ICCV_2025_paper.html), pages 20147–20156, 2025.
- [17] Changxu Duan, Zhiyin Tan, and Sabine Bartsch. LaTeX rainbow: Universal LaTeX to PDF document semantic & layout annotation framework. In [Proceedings of the Second Workshop on Information Extraction from Scientific Publications](https://openaccess.thecvf.com/content_Proceedings_of_the_Second_Workshop_on_Information_Extraction_from_Scientific_Publications_2023.html), pages 56–67, 2023.
- [18] Shancheng Fang, Hongtao Xie, Yuxin Wang, Zhendong Mao, and Yongdong Zhang. Read like humans: Autonomous, bidirectional and iterative language modeling for scene text recognition. In [CVPR](https://openaccess.thecvf.com/content_CVPR_2021/html/Fang_Read_Like_Humans_Autonomous_Bidirectional_and_Iterative_Language_Modeling_for_Scene_Text_Recognition_CVPR_2021_paper.html), pages 7098–7107, 2021.
- [19] Shancheng Fang, Zhendong Mao, Hongtao Xie, Yuxin Wang, Chenggang Yan, and Yongdong Zhang. ABINet++: Autonomous, bidirectional and iterative language modeling for scene text spotting. [IEEE Trans. Pattern Anal. Mach. Intell.](https://ieeexplore.ieee.org/abstract/document/9545453), 45(6):7123–7141, 2023.

[20] Hao Feng, Shu Wei, Xiang Fei, Wei Shi, Yingdong Han, Lei Liao, Jinghui Lu, Binghong Wu, Qi Liu, Chunhui Lin, et al. Dolphin: Document image parsing via heterogeneous anchor prompting. [arXiv preprint arXiv:2505.14059](https://arxiv.org/abs/2505.14059), 2025.

[21] Filimoa. open-parse. <https://github.com/Filimoa/open-parse>, 2024. Accessed: 2025-06-23.

[22] Google DeepMind. Gemini 2.5. <https://blog.google/technology/google-deepmind/gemini-model-thinking-updates-march-2025/>, 2025.

[23] Alex Graves, Santiago Fernández, Faustino Gomez, and Jürgen Schmidhuber. Connectionist temporal classification: Labelling unsegmented sequence data with recurrent neural networks. In [ICML](https://icml.cc/2006/paper/369.pdf), pages 369–376, 2006.

[24] Tongkun Guan, Wei Shen, Xue Yang, Qi Feng, Zekun Jiang, and Xiaokang Yang. Self-Supervised Character-to-Character distillation for text recognition. In [ICCV](https://iccv.org/2023/paper/19473.pdf), pages 19473–19484, 2023.

[25] Dong Guo, Faming Wu, Feida Zhu, Fuxing Leng, Guang Shi, Haobin Chen, Haoqi Fan, Jian Wang, Jianyu Jiang, Jiawei Wang, et al. Seed1. 5-vl technical report. [arXiv preprint arXiv:2505.07062](https://arxiv.org/abs/2505.07062), 2025.

[26] Mengchao He, Yuliang Liu, Zhibo Yang, Sheng Zhang, Canjie Luo, Feiyu Gao, Qi Zheng, Yongpan Wang, Xin Zhang, and Lianwen Jin. ICPR2018 contest on robust reading for multi-type web images. In [ICPR](https://icpr.org/2018/paper/7-12.pdf), pages 7–12, 2018.

[27] Wenyang Hu, Xiaocong Cai, Jun Hou, Shuai Yi, and Zhiping Lin. Gtc: Guided training of ctc towards efficient and accurate scene text recognition. In [AAAI](https://aaai.org/AAAI-20/paper/11005.pdf), volume 34, pages 11005–11012, 2020.

[28] Geewook Kim, Teakgyu Hong, Moonbin Yim, JeongYeon Nam, Jinyoung Park, Jinyeong Yim, Wonseok Hwang, Sangdoo Yun, Dongyoon Han, and Seunghyun Park. Ocr-free document understanding transformer. In [ECCV](https://eccv.org/2022/paper/498-517.pdf), pages 498–517. Springer, 2022.

[29] Hui Li, Peng Wang, Chunhua Shen, and Guyu Zhang. Show, attend and read: A simple and strong baseline for irregular text recognition. In [AAAI](https://aaai.org/AAAI-19/paper/8610.pdf), pages 8610–8617, 2019.

[30] Yumeng Li, Guang Yang, Hao Liu, Bowen Wang, and Colin Zhang. dots.ocr: Multilingual document layout parsing in a single vision-language model, 2025.

[31] Zhang Li, Yuliang Liu, Qiang Liu, Zhiyin Ma, Ziyang Zhang, Shuo Zhang, Zidun Guo, Jiarui Zhang, Xinyu Wang, and Xiang Bai. Monkeyocr: Document parsing with a structure-recognition-relation triplet paradigm. [arXiv preprint arXiv:2506.05218](https://arxiv.org/abs/2506.05218), 2025.

[32] Aixin Liu, Bei Feng, Bin Wang, Bingxuan Wang, Bo Liu, Chenggang Zhao, Chengqi Deng, Chong Ruan, Damai Dai, Daya Guo, et al. Deepseek-v2: A strong, economical, and efficient mixture-of-experts language model. [arXiv preprint arXiv:2405.04434](https://arxiv.org/abs/2405.04434), 2024.

[33] Cheng-Lin Liu, Fei Yin, Da-Han Wang, and Qiu-Feng Wang. Casia online and offline chinese handwriting databases. In [ICDAR](https://icdar.org/2011/paper/37-41.pdf), pages 37–41, 2011.

[34] Yuliang Liu, Biao Yang, Qiang Liu, Zhang Li, Zhiyin Ma, Shuo Zhang, and Xiang Bai. Textmonkey: An ocr-free large multimodal model for understanding document. [arXiv preprint arXiv:2403.04473](https://arxiv.org/abs/2403.04473), 2024.

[35] Shangbang Long, Siyang Qin, Dmitry Panteleev, Alessandro Bissacco, Yasuhisa Fujii, and Michalis Raptis. Towards end-to-end unified scene text detection and layout analysis. In [CVPR](https://cvpr.org/2022/paper/1049-1059.pdf), pages 1049–1059, 2022.

[36] Ilya Loshchilov and Frank Hutter. Decoupled weight decay regularization. In [ICLR](https://iclr.cc/2019/paper/12.pdf), 2019.

[37] Lukas Blecher. pix2tex - latex ocr. <https://github.com/lukas-blecher/LaTeX-OCR>, 2022. Accessed: 2025-06-23.

[38] Canjie Luo, Lianwen Jin, and Zenghui Sun. MORAN: A multi-object rectified attention network for scene text recognition. [Pattern Recognit.](https://www.ncbi.nlm.nih.gov/pmc/articles/PMC7000000/), 90:109–118, 2019.

[39] Souvik Mandal, Ashish Talewar, Paras Ahuja, and Prathamesh Juvatkar. Nanonets-ocr-s: A model for transforming documents into structured markdown with intelligent content recognition and semantic tagging, 2025.

[40] Mathpix. Mathpix snip: Convert images and pdfs to latex, docx, and more. <https://mathpix.com/>, 2025.

[41] Ahmed Nassar, Andres Marafioti, Matteo Omenetti, Maksym Lysak, Nikolaos Livathinos, Christoph Auer, Lucas Morin, Rafael Teixeira de Lima, Yusik Kim, A Said Gurbuz, et al. Smoldocling: An ultra-compact vision-language model for end-to-end multi-modal document conversion. [arXiv preprint arXiv:2503.11576](https://arxiv.org/abs/2503.11576), 2025.

[42] Junbo Niu, Zheng Liu, Zhuangcheng Gu, Bin Wang, Linke Ouyang, Zhiyuan Zhao, Tao Chu, Tianyao He, Fan Wu, Qintong Zhang, et al. Mineru2. 5: A decoupled vision-language model for efficient high-resolution document parsing. [arXiv preprint arXiv:2509.22186](https://arxiv.org/abs/2509.22186), 2025.

[43] opendatalab. Mineru2.0-2505-0.9b. <https://huggingface.co/opendatalab/MinerU2.0-2505-0.9B>, 2025.

[44] Linke Ouyang, Yuan Qu, Hongbin Zhou, Jiawei Zhu, Rui Zhang, Qunshu Lin, Bin Wang, Zhiyuan Zhao, Man Jiang, Xiaomeng Zhao, et al. Omnidocbench: Benchmarking diverse pdf document parsing with comprehensive annotations. In [CVPR](https://cvpr2025.org/), pages 24838–24848, 2025.

[45] Vik Paruchuri. Marker. <https://github.com/datalab-to/marker>, 2025. Accessed: 2025-09-25.

[46] Jake Poznanski, Jon Borchardt, Jason Dunkelberger, Regan Huff, Daniel Lin, Aman Rangapur, Christopher Wilhelm, Kyle Lo, and Luca Soldaini. olmocr: Unlocking trillions of tokens in pdfs with vision language models. [arXiv preprint arXiv:2502.18443](https://arxiv.org/abs/2502.18443), 2025.

[47] Fenfen Sheng, Zhiheng Chen, and Bo Xu. NRTR: A no-recurrence sequence-to-sequence model for scene text recognition. In [ICDAR](https://icdar.org/), pages 781–786, 2019.

[48] Baoguang Shi, Xiang Bai, and Cong Yao. An end-to-end trainable neural network for image-based sequence recognition and its application to scene text recognition. [IEEE Trans. Pattern Anal. Mach. Intell.](https://ieeexplore.ieee.org/abstract/document/8307571), 39(11):2298–2304, 2017. doi: 10.1109/TPAMI.2016.2646371.

[49] Baoguang Shi, Mingkun Yang, Xinggang Wang, Pengyuan Lyu, Cong Yao, and Xiang Bai. ASTER: An attentional scene text recognizer with flexible rectification. [IEEE Trans. Pattern Anal. Mach. Intell.](https://ieeexplore.ieee.org/abstract/document/8750510), 41(9):2035–2048, 2019.

[50] Yipeng Sun, Zihan Ni, Chee-Kheng Chng, Yuliang Liu, Canjie Luo, Chun Chet Ng, Junyu Han, Errui Ding, Jingtuo Liu, Dimosthenis Karatzas, Chee Seng Chan, and Lianwen Jin. ICDAR 2019 competition on large-scale street view text with partial labeling-rrc-lsvt. In [ICDAR](https://icdar.org/), pages 1557–1562, 2019.

[51] TAL. Tal open dataset. <https://ai.100tal.com/dataset>, 2023.

[52] Docling Team. Docling. <https://github.com/docling-project/docling>, 2024. Accessed: 2025-06-23.

[53] Hunyuan Vision Team, Pengyuan Lyu, Xingyu Wan, Gengluo Li, Shangpin Peng, Weinong Wang, Liang Wu, Huawei Shen, Yu Zhou, Canhui Tang, Qi Yang, Qiming Peng, Bin Luo, Hower Yang, Xinsong Zhang, Jinnian Zhang, Houwen Peng, Hongming Yang, Senhao Xie, Longsha Zhou, Ge Pei, Binghong Wu, Rui Yan, Kan Wu, Jieneng Yang, Bochao Wang, Kai Liu, Jianchen Zhu, Jie Jiang, Linus, Han Hu, and Chengquan Zhang. Hunyuanocr technical report, 2025.

[54] Kimi Team, Angang Du, Bohong Yin, Bowei Xing, Bowen Qu, Bowen Wang, Cheng Chen, Chenlin Zhang, Chenzhuang Du, Chu Wei, et al. Kimi-vl technical report. [arXiv preprint arXiv:2504.07491](https://arxiv.org/abs/2504.07491), 2025.

[55] Tencent. Hunyuan-0.5b. <https://github.com/Tencent-Hunyuan/Hunyuan-0.5B>, 2025.

[56] Unstructured-IO. unstructured. <https://github.com/Unstructured-IO/unstructured>, 2022. Accessed: 2025-06-23.

[57] Ilya Loshchilov and Frank Hutter. SGDR: stochastic gradient descent with warm restarts. In [ICLR](https://iclr.cc/2017/), 2017.

[58] Bin Wang, Zhuangcheng Gu, Guang Liang, Chao Xu, Bo Zhang, Botian Shi, and Conghui He. UniMERNNet: A universal network for real-world mathematical expression recognition. [arXiv preprint arXiv:2404.15254](https://arxiv.org/abs/2404.15254), 2024.

[59] Bin Wang, Chao Xu, Xiaomeng Zhao, Linke Ouyang, Fan Wu, Zhiyuan Zhao, Rui Xu, Kaiwen Liu, Yuan Qu, Fukai Shang, et al. Mineru: An open-source solution for precise document content extraction. [arXiv preprint arXiv:2409.18839](https://arxiv.org/abs/2409.18839), 2024.

[60] Peng Wang, Cheng Da, and Cong Yao. Multi-Granularity Prediction for scene text recognition. In [ECCV](https://eccv2022.org/), pages 339–355, 2022.

[61] Yuxin Wang, Hongtao Xie, Shancheng Fang, Mengting Xing, Jing Wang, Shenggao Zhu, and Yongdong Zhang. PETR: Rethinking the capability of transformer-based language model in scene text recognition. [IEEE Trans. Image Process.](https://ieeexplore.ieee.org/abstract/document/9790003), 31:5585–5598, 2022.

[62] Haoran Wei, Chenglong Liu, Jinyue Chen, Jia Wang, Lingyu Kong, Yanming Xu, Zheng Ge, Liang Zhao, Jianjian Sun, Yuang Peng, et al. General ocr theory: Towards ocr-2.0 via a unified end-to-end model. [arXiv preprint arXiv:2409.01704](#), 2024.

[63] Haoran Wei, Yaofeng Sun, and Yukun Li. Deepseek-ocr: Contexts optical compression. [arXiv preprint arXiv:2510.18234](#), 2025.

[64] Jin-Wen Wu, Fei Yin, Yan-Ming Zhang, Xu-Yao Zhang, and Cheng-Lin Liu. Handwritten mathematical expression recognition via paired adversarial learning. *IJCV*, 128:2386–2401, 2020.

[65] An Yang, Anfeng Li, Baosong Yang, Beichen Zhang, Binyuan Hui, Bo Zheng, Bowen Yu, Chang Gao, Chengan Huang, Chenxu Lv, et al. Qwen3 technical report. [arXiv preprint arXiv:2505.09388](#), 2025.

[66] Biao Yang, Bin Wen, Boyang Ding, Changyi Liu, Chenglong Chu, Chengru Song, Chongling Rao, Chuan Yi, Da Li, Dunju Zang, et al. Kwai keye-vl 1.5 technical report. [arXiv preprint arXiv:2509.01563](#), 2025.

[67] Jianwei Yang, Chunyuan Li, Xiyang Dai, and Jianfeng Gao. Focal modulation networks. In [NeurIPS](#), pages 4203–4217, 2022.

[68] Deli Yu, Xuan Li, Chengquan Zhang, Junyu Han, Jingtuo Liu, and Errui Ding. Towards accurate scene text recognition with semantic reasoning networks. In [CVPR](#), pages 12113–12122, 2020.

[69] Xiaoyu Yue, Zhanghui Kuang, Chenhao Lin, Hongbin Sun, and Wayne Zhang. RobustScanner: Dynamically enhancing positional clues for robust text recognition. In [ECCV](#), pages 135–151, 2020.

[70] Jianshu Zhang, Jun Du, Shiliang Zhang, Dan Liu, Yulong Hu, Jinshui Hu, Si Wei, and Lirong Dai. Watch, attend and parse: An end-to-end neural network based approach to handwritten mathematical expression recognition. *PR*, 71:196–206, 2017.

[71] Jianshu Zhang, Jun Du, Yongxin Yang, Yi-Zhe Song, Si Wei, and Lirong Dai. A tree-structured decoder for image-to-markup generation. In [ICML](#), pages 11076–11085. PMLR, 2020.

[72] Qintong Zhang, Bin Wang, Victor Shea-Jay Huang, Junyuan Zhang, Zhengren Wang, Hao Liang, Conghui He, and Wentao Zhang. Document parsing unveiled: Techniques, challenges, and prospects for structured information extraction. [arXiv preprint arXiv:2410.21169](#), 2024.

[73] Shuai Zhao, Yongkun Du, Zhineng Chen, and Yu-Gang Jiang. Decoder pre-training with only text for scene text recognition. In [ACM MM](#), pages 5191–5200, 2024. ISBN 9798400706868.

[74] Shuai Zhao, Ruijie Quan, Linchao Zhu, and Yi Yang. CLIP4STR: A simple baseline for scene text recognition with pre-trained vision-language model. *IEEE Trans. Image Process.*, 33:6893–6904, 2024.

[75] Zhen Zhao, Jingqun Tang, Chunhui Lin, Binghong Wu, Can Huang, Hao Liu, Xin Tan, Zhizhong Zhang, and Yuan Xie. Multi-modal in-context learning makes an ego-evolving scene text recognizer. In [CVPR](#), pages 15567–15576, 2024.

[76] Tianlun Zheng, Zhineng Chen, Shancheng Fang, Hongtao Xie, and Yu-Gang Jiang. CDistNet: Perceiving multi-domain character distance for robust text recognition. *Int. J. Comput. Vis.*, 132(2):300–318, 2024.

[77] Humen Zhong, Zhibo Yang, Zhaohai Li, Peng Wang, Jun Tang, Wenqing Cheng, and Cong Yao. VL-reader: Vision and language reconstructor is an effective scene text recognizer. In [ACM MM](#), pages 4207–4216, 2024.

[78] Jinguo Zhu, Weiyun Wang, Zhe Chen, Zhaoyang Liu, Shenglong Ye, Lixin Gu, Hao Tian, Yuchen Duan, Weijie Su, Jie Shao, et al. Internvl3: Exploring advanced training and test-time recipes for open-source multimodal models. [arXiv preprint arXiv:2504.10479](#), 2025.

Appendix

More Recognition Result Visualizations

To illustrate the recognition cases of our proposed UniRec-0.1B alongside existing models, we present several representative qualitative examples across diverse scenarios. These include mixed Chinese text with inline formulas, clean printed text, handwritten notes, and multi-line formulas, covering key challenges commonly encountered in real-world documents. As shown in Fig. 5, we present an example of multi-line Chinese text containing inline formulas. Fig. 6 illustrates three clean and straightforward recognition results. Fig. 7 provides two examples of multi-line handwritten text, while Fig. 8 displays a multi-line formula recognition case. Fig. 9 highlights two typical failure cases of UniRec-0.1B. Finally, Fig. 10 and Fig. 11 illustrate the page-level recognition results of UniRec-0.1B. Through these concrete comparisons, we emphasize the strengths of our method and characterize common failure modes of existing models, thereby complementing quantitative evaluations and offering more intuitive insights into the practical performance of each approach.

Label:

[答案]:B [解析]: 【解析】因为 $f'(0)=m$ ，所以 $f(x)$ 在 $x=0$ 处连续，从而 $\lim_{x \rightarrow 0} f(x) = f(0) = 0$ ，所以 $\lim_{x \rightarrow 0} \frac{f(x) - f(0)}{x} = \lim_{x \rightarrow 0} \frac{f(x) - 0}{x} = m$ ，故选 B。
对于 A 选项， $\lim_{x \rightarrow 0} f(x) = m$ ，推不出来 $f'(0)=m$ ；对于 C 选项， $f'(x)$ 在 $x=0$ 处不一定连续；对于 D 选项， $f'(x)$ 在 $x=0$ 处极限未必存在。

UniRec-0.1B:

[答案]:B [解析]: 【解析】因为 $f'(0)=m$ ，所以 $f(x)$ 在 $x=0$ 处连续，从而 $\lim_{x \rightarrow 0} f(x) = f(0) = 0$ ，所以 $\lim_{x \rightarrow 0} \frac{f(x) - f(0)}{x} = \lim_{x \rightarrow 0} \frac{f(x) - 0}{x} = m$ ，故选 B。

对于 A 选项， $\lim_{x \rightarrow 0} f(x) = m$ ，推不出来 $f'(0)=m$ ；对于 C 选项， $f'(x)$ 在 $x=0$ 处不一定连续；对于 D 选项， $f'(x)$ 在 $x=0$ 处极限未必存在。

Dolphin-1.5-3B:

[答案]:B [解析]: 【解析】因为 $f'(0) = m$ ，所以 $f(x)$ 在 $x=0$ 处连续，从而 $\lim_{x \rightarrow 0} f(x) = f(0) = 0$ ，所以

$x \rightarrow 0$
 $f(x) = f(0) = 0$ ，所以

$\lim_{x \rightarrow 0} f(x) = 0$

$f(x) = f(0)$

$x = 0$

Ⓐ $\sqrt[3]{7c}$
Ⓑ $\sqrt[7]{12d}$
Ⓒ $3\sqrt[4]{5f}$

Label:

$\$ \text{textcircled}{a} \$ \$ \sqrt{3}[7c] \$ \n \$ \text{textcircled}{b} \$ \$ \sqrt{7}[12d] \$ \n \$ \text{textcircled}{c} \$ \$ 3\sqrt{4}[5f] \$$

UniRec-0.1B:

$\backslash \text{textcircled}{a} \sqrt{3}[7c] \backslash$
 $\backslash \text{textcircled}{b} \sqrt{7}[12d] \backslash$
 $\backslash \text{textcircled}{c} 3\sqrt{4}[5f] \backslash$

Dolphin-1.5-0.3B:

$\$ \sqrt[3]{3}[7c] \$$
 $\$ \sqrt[3]{3}[12d] \$$
 $\$ 3\sqrt[4]{5f} \$$

PaddleOCR-VL-0.9B:

$_a \$ \sqrt{3}[7c] \$$
 $_b \$ \sqrt{7}[12d] \$$
 $_c \$ 3\sqrt{4}[5f] \$$

MinerU2.5 -1.2B:

$\backslash (\text{text}{a}) \sqrt{3}[7c] \backslash \backslash (\text{text}{b}) \sqrt{7}[12d] \backslash \backslash (\text{text}{c}) 3\sqrt{4}[5f] \backslash$

MonkeyOCR-pro-3B:

$_a \$ 3\sqrt{3}[7c] \$$
 $_b \$ \sqrt{7}[12d] \$$
 $_c \$ 3 \$ \sqrt{4}[5f] \$$

dots.ocr-3B:

a) $\$ \sqrt{3}[7c] \$$
b) $\$ \sqrt{7}[12d] \$$
c) $\$ \sqrt{3}[5f^4] \$$

Nanonets-OCR2-3B:

$\text{<table> <thead> <tr> <td> a </td> <td> b </td> <td> c </td> </tr> <tbody> <tr> <td> 3\sqrt[3]{7c} </td> <td> 3\sqrt[7]{12d} </td> <td> 3\sqrt[4]{5f} </td> </tr> </tbody> </table>$
- a) $\sqrt{3}[7c]$
- b) $\sqrt{7}[12d]$
- c) $\sqrt{4}[5f]$

In order to test the sensitivity of the solution on the parameter σ_e , the dissimilarity map given by the

Label:

In order to test the sensitivity of the solution on the parameter $\$ \sigma_e \$$, the dissimilarity map given by the

UniRec-0.1B:

In order to test the sensitivity of the solution on $\$ \sigma_e \$$, the dissimilarity map given by the

Dolphin-1.5-0.3B:

In order to test the sensitivity of the solution on the parameter $\$ \sigma_e \$$, the dissimilarity map given by the

PaddleOCR-VL-0.9B:

In order to test the sensitivity of the solution on the parameter $\$ \sigma_e \$$, the dissimilarity map given by the

MinerU2.5 -1.2B:

In order to test the sensitivity of the solution on the parameter $\$ \sigma_e \$$, the dissimilarity map given by the

6. The table shows the number of bills of each value that Bree received for her birthday. In all, what fraction of the number of bills that Bree received for her birthday were \$10 or \$20 bills?

Label:

6. The table shows the number of bills of each value that Bree received for her birthday. In all, what fraction of the number of bills that Bree received for her birthday were \$10 or \$20 bills?

UniRec-0.1B:

6. The table shows the number of bills of each value that Bree received for her birthday. In all, what fraction of the number of bills that Bree received for her birthday were \$10 or \$20 bills?

Dolphin-1.5-0.3B:

6. The table shows the number of bills of each value that Bree received for her birthday. In all, what fraction of the number of bills that Bree received for her birthday were \$10 or \$20 bills?

PaddleOCR-VL-0.9B:

6. The table shows the number of bills of each value that Bree received for her birthday. In all, what fraction of the number of bills that Bree received for her birthday were \$10 or \$20 bills?

MinerU2.5 -1.2B:

6. The table shows the number of bills of each value that Bree received for her birthday. In all, what fraction of the number of bills that Bree received for her birthday were \$10 or \$20 bills?

MonkeyOCR-pro-3B:

6. The table shows the number of bills of each value that Bree received for her birthday. In all, what fraction of the number of bills that Bree received for her birthday were \$10 or \$20 bills?

dots.ocr-3B:

6. The table shows the number of bills of each value that Bree received for her birthday. In all, what fraction of the number of bills that Bree received for her birthday were \$10 or \$20 bills?

Nanonets-OCR2-3B:

$\$ \frac{3}{7} \$$

DeepSeek-OCR-3B :

6. The table shows the number of bills of each value that Bree received for her birthday. In all, what fraction of the number of bills that Bree received for her birthday were \$10 or \$20 bills?

Figure 6 Results for three clean and simple examples. Most methods correctly recognize the content. In the first example, all methods except UniRec-0.1B misrecognize Ⓐ, Ⓑ, and Ⓒ as the plain characters “a”, “b”, and “c”. In the second example, only Nanonets-OCR2 exhibits severe errors, producing outputs entirely unrelated to the image. In the third example, Dolphin-1.5, PaddleOCR-VL, and DeepSeek-OCR fail to capture the correct style of the character “e”, while MonkeyOCR incorrectly predicts it as “c”. **Red characters** denote recognition errors, **_** marks missing characters, and **green text** indicates correct recognition.

Label:

例如: 只有当你书图(如世界气候类型分布图)结合进行复习, 掌握了影响气候的各种因素和世界各主要气候类型的特点, 分布规律和形成原因等基础知识要点, 同时又掌握了气温、降水等各种气候资料、图表的含义, 制作与使用方法等基本技能, 才有可能根据有关的气候资料、图表(如各月或一、七月和全年气温、降水数字资料、各月气温变化曲线和降水分配柱状图等)或某地的纬度位置、海陆位置、地形特点等, 对其气候类型作出正确的判断和解答来。否则, 是不可能的。

UniRec-0.1B:

例如: 只有当你书图(如世界气候类型分布图)结合进行复习, 掌握了影响气候的各种因素和世界各主要气候类型的特点, 分布规律和形成原因等基础知识要点, 同时又掌握了气温、降水等各种气候资料、图表的含义, 制作与使用方法等基本技能, 才有可能根据有关的气候资料、图表(如各月或一、七月和全年气温、降水数字资料、各月气温变化曲线和降水分配柱状图等)或某地的纬度位置、海陆位置、地形特点等, 对其气候类型作出正确的判断和解答来。否则, 是不可能的。

Dolphin-1.5-0.3B:

例如: 只有当你书图(如世界气候类型分布图)结合 **独行复旦**, 掌握了影响气候的各种因素和世界各主要气候类型的特点、分布规律和形成原因等基础知识要点。同时又掌握 **飞去温降水** **准备钟步便爱学园** 表的含义, 制作与使用方法 **尊重本技能才** 有可能根据有关的气候 **类资料** **围绕**(如各月或一、七月和全年 **发掘**, 降水数字资料、各 **涵** 变化曲线和降水分配 **样状图等**)或某地的纬度位置、海陆 **应置**、**加热**特点 **象** 对其气候类型 **下也** 正确的判断和 **屏需求**。否则, 是不可能的。

例如: 只有当你书图(如世界气候类型分布图)结合进行复习, 掌握了影响气候的各种因素和世界各主要气候类型的特点, 分布规律和形成原因等基础知识要点, 同时又掌握了气温、降水等各种气候资料、图表的含义, 制作与使用方法等基本技能, 才有可能根据有关的气候资料、图表(如各月或一、七月和全年气温、降水数字资料、各月气温变化曲线和降水分配柱状图等)或某地的纬度位置、海陆位置、地形特点等, 对其气候类型作出正确的判断和解答来。否则, 是不可能的。

PaddleOCR-VL-0.9B:

例如: 只有当你书图(如世界气候类型分布图)结合进行复习, 掌握了影响气候的各种因素和世界各主要气候类型的特点, 分布规律和形成原因等基础知识要点, 同时 **掌握** 气温降水等各种气候资料、图表的含义, 制作与使用方法等基本技能, 才有可能根据有关的气候资料、图表(如各月或一、七月和全年气温、降水数字资料、各月气温变化曲线和降水分配柱状图等)或某地的纬度位置、海陆位置、地形特点等, 对其气候类型作出正确的判断和解答来。否则, 是不可能的。

MinerU2.5-1.2B:

例如: 只有当 **水汽圈**(如世界气候类型分布图)结合进行复习, 掌握了影响气候的各种因素和世界各主要气候类型的特点, 分布规律和 **成因成因** 等基础知识 **总和**, 同时又掌握了气温、降水等各种气候资料、图表的含义, 制作与使用方法等基本技能, 才有可能根据有关的气候 **条件**、**风**、**霜**(各月或一、七月和全年气温、降水等)资料, 各种气温变化曲线和降水分配 **挂水图等** 或某地的纬度位置、海陆位置、地形特点等, 对其气候 **条件** 正确的判断和 **判断来**。否则, 是不可能的。

MonkeyOCR-pro-3B:

例如: 只有当您知道(世界气候分布分布)结合进行 **最易考虑** 了影响气候的各种因素和 **距陆表** 主要气候类型的特点, 分析 **风向和雨成原因等** 知识要多, 同时 **仅掌握** 气温、降水、**湿度等** 综合因素, 制作与使用方法等基本技能, 才能 **准确地** 根据有关的气候资料, **确定**(如 **月均** 或一月上旬、下旬)某地区, 进而 **掌握各要素间关系变化** 和 **降水分配情况**。某地区的纬度位置、海陆位置, **以及地理位置** 对 **当地气候的影响** 作出正确的判断和 **预测来**。否则, 是不可能的。

dotsOCR-3B:

例如: 只有当你书图(如世界气候类型分布图)结合进行复习, 掌握了影响气候的各种因素和世界各主要气候类型的特点, 分布规律和形成原因等基础知识要点, 同时又掌握了气温、降水等各种气候资料、图表的含义, 制作与使用方法等基本技能, 才有可能根据有关的气候资料、图表(如各月或一、七月和全年气温、降水数字资料, 各 **形成地区** 变化曲线和降水分配 **在状图等**)或某地的纬度位置、海陆位置、地形特点等, 对其气候类型作出正确的判断和 **分析来**。否则, 是不可能的。

Nanonet-OCR2-3B:

例如: 只有当 **气候圈**(如世界气候类型分布图)结合 **往期气象** 掌握了影响气候的各种因素和世界主要气候类型的特点、分析规律和形成原因等基础知识要点。同时又掌握 **交通、旅游** 等各种气候资料、图表的含义, 制作与使用方法等基本技能, 才能有可能根据有关的气候资料, **绘制**(如每月或一月、七月 **平均气温**、**降水次数** 资料, 各月 **温度** 变化曲线和 **年平均水汽压等数据**)或某地的纬度位置、海拔位置、**日照特点** **总结** 对其气候类型作出正确的判断和 **预测**。否则, 是不可能的。

DeepSeek-OCR-3B:

例如: 只有当 **您手** 图(如世界气候类型分布图)结合进行复习, 掌握了影响气候的各种因素和世界各主要气候类型的特点, 分布规律和形成原因等基础知识要点, 同时又掌握 **交通、旅游** 等各种气候资料、图表的含义, 制作与使用方法等基本技能, 才有可能根据有关的资料、图表(如各月或一月和全年气温、降水数字资料、各月 **降水量** 变化曲线和降水分配柱状图等)或某地的纬度位置、海陆位置、地形特点等, 对其气候类型作出正确的判断和 **回答**。否则, 是不可能的。

To sum up, we should try to bring the advantage of **17/18** into full play and reduce the disadvantage to the minimum at the same time. In that case, we will definitely make a better use of the **讨论议题**.

MinerU2.5-1.2B:

To sum up, we should try to bring the advantage of **ititie again** into full play and reduce the disadvantage to the minimum at the same time. In that case, we will definitely make a better use of the **ititie again**.

Label:

To sum up, we should try to bring the advantage of **讨论议题** into full play, and reduce the disadvantage to the minimum at the same time. In that case, we will definitely make a better use of the **讨论议题**.

UniRec-0.1B:

To sum up, we should try to bring the advantage of **讨论议题** into full play, and reduce the disadvantage to the minimum at the same time. In that case, we will definitely make a better use of the **讨论议题**.

Dolphin-1.5-0.3B:

To sum up, we should try to bring the advantage of **little like** into full play and reduce the disadvantage to the minimum at the same time. In that case, we will definitely make a better use of the **title or for**.

MonkeyOCR-pro-3B:

To sum up, we should try to bring the advantage of **\$** into full play and reduce the disadvantage to the minimum at the same time. In that case, we will definitely make a better use of the **\$ resources**.

PaddleOCR-VL-0.9B:

To sum up, we should try to bring the advantage of **讨论议题** into full play, and reduce the disadvantage to the minimum at the same time. In that case, we will definitely make a better use of the **讨论议题**.

dotsOCR-3B:

To sum up, we should try to bring the advantage of **17/18** into full play, and reduce the disadvantage to the minimum at the same time. In that case, we will definitely make a better use of the **advantage**.

Nanonet-OCR2-3B:

To sum up, we should try to bring the advantage of **the system**

DeepSeek-OCR-3B:

To sum up, we should try to bring the advantage of **其他议题** into full play, and reduce the disadvantage to the minimum at the same time. In that case, we will definitely make a better use of the **其他议题**.

Figure 7 Results for two multi-line handwritten text examples. For the Chinese handwriting case, UniRec-0.1B achieves perfect recognition, followed by PaddleOCR-VL, which misses a few characters. All other methods produce substantial errors, consistent with their significantly worse edit-distance performance on the note subset. For the multi-line English handwriting example, a similar pattern emerges: only UniRec-0.1B and PaddleOCR-VL correctly recognize the text. All other methods fail to identify the few embedded Chinese characters. **Red characters** indicate recognition errors and **Green** indicates correct recognition.

$$\begin{aligned}
-a^{ij}w_{x_i x_j} &= \frac{-a^{ij}u_{x_i x_j}v + a^{ij}v_{x_i x_j}u}{v^2} + \frac{a^{ij}v_{x_i}u_{x_j} - a^{ij}u_{x_i}v_{x_j}}{v^2} - a^{ij}\frac{2}{v}v_{x_j}\frac{v_{x_i}u - vu_{x_i}}{v^2} \\
&= \frac{(Lu - b^i u_{x_i} - cu)v + (-Lv + b^i v_{x_i} + cv)u}{v^2} + 0 + a^{ij}\frac{2}{v}v_{x_j}w_{x_i}, \text{ since } a^{ij} = a^{ji}. \\
&= \frac{Lu}{v} - \frac{uLv}{v^2} - b^i w_{x_i} + a^{ij}\frac{2}{v}v_{x_j}w_{x_i}
\end{aligned}$$

UniRec-0.1B:

$$\begin{aligned}
-a^{ij}w_{x_i x_j} &= \frac{-a^{ij}u_{x_i x_j}v + a^{ij}v_{x_i x_j}u}{v^2} + \frac{a^{ij}v_{x_i}u_{x_j} - a^{ij}u_{x_i}v_{x_j}}{v^2} - a^{ij}\frac{2}{v}v_{x_j}\frac{v_{x_i}u - vu_{x_i}}{v^2} \\
&= \frac{(Lu - b^i u_{x_i} - cu)v + (-Lv + b^i v_{x_i} + cv)u}{v^2} + 0 + a^{ij}\frac{2}{v}v_{x_j}w_{x_i}, \text{ since } a^{ij} = a^{ji}. \\
&= \frac{Lu}{v} - \frac{uLv}{v^2} - b^i w_{x_i} + a^{ij}\frac{2}{v}v_{x_j}w_{x_i}
\end{aligned}$$

Dolphin-1.5-0.3B:

$$\begin{aligned}
-a^{ij}w_{x_i x_j} &= \frac{-a^{ij}u_{x_i x_j}v + a^{ij}v_{x_i x_j}u}{v^2} + \frac{a^{ij}v_{x_i}u_{x_j} - a^{ij}u_{x_i}v_{x_j}}{v^2} - a^{ij}\frac{2}{v}v_{x_j}\frac{v_{x_i}u - vu_{x_i}}{v^2} \\
&= \frac{(Lu - b^i u_{x_i} - cu)v + (-Lv + b^i v_{x_i} + cv)u}{v^2} + 0 + a^{ij}\frac{2}{v}v_{x_j}w_{x_i}, \text{ since } a^{ij} = a^{ji}. \\
&= \frac{Lu}{v} - \frac{uLv}{v^2} - b^i w_{x_i} + a^{ij}\frac{2}{v}v_{x_j}w_{x_i}
\end{aligned}$$

PaddleOCR-VL-0.9B:

$$\begin{aligned}
-a^{ij}w_{x_i x_j} &= \frac{-a^{ij}u_{x_i x_j}v + a^{ij}v_{x_i x_j}u}{v^2} + \frac{a^{ij}v_{x_i}u_{x_j} - a^{ij}u_{x_i}v_{x_j}}{v^2} - a^{ij}\frac{2}{v}v_{x_j}\frac{v_{x_i}u - vu_{x_i}}{v^2} \equiv \\
&= \frac{(Lu - b^i u_{x_i} - cu)v + (-Lv + b^i v_{x_i} + cv)u}{v^2} + 0 + a^{ij}\frac{2}{v}v_{x_j}w_{x_i}, \text{ since } a^{ij} = a^{ji}. = \frac{Lu}{v} - \frac{uLv}{v^2} - b^i w_{x_i} + a^{ij}\frac{2}{v}v_{x_j}w_{x_i}
\end{aligned}$$

MinerU2.5 -1.2B:

$$\begin{aligned}
-a^{ij}w_{x_i x_j} &= \frac{-a^{ij}u_{x_i x_j}v + a^{ij}v_{x_i x_j}u}{v^2} + \frac{a^{ij}v_{x_i}u_{x_j} - a^{ij}u_{x_i}v_{x_j}}{v^2} - a^{ij}\frac{2}{v}v_{x_j}\frac{v_{x_i}u - vu_{x_i}}{v^2} \\
&= \frac{(Lu - b^i u_{x_i} - cu)v + (-Lv + b^i v_{x_i} + cv)u}{v^2} + 0 + a^{ij}\frac{2}{v}v_{x_j}w_{x_i}, \text{ since } a^{ij} = a^{ji}.
\end{aligned}$$

MonkeyOCR-pro-3B:

$$\begin{aligned}
-a^{ij}w_{x_i x_j} &= \frac{-a^{ij}u_{x_i x_j}v + a^{ij}v_{x_i x_j}u}{v^2} + \frac{a^{ij}v_{x_i}u_{x_j} - a^{ij}u_{x_i}v_{x_j}}{v^2} - a^{ij}\frac{2}{v}v_{x_j}\frac{v_{x_i}u - vu_{x_i}}{v^2} \\
&= \frac{(Lu - b^i u_{x_i} - cu)v + (-Lv + b^i v_{x_i} + cv)u}{v^2} + 0 + a^{ij}\frac{2}{v}v_{x_j}w_{x_i}, \text{ since } a^{ij} = a^{ji}.
\end{aligned}$$

dots.ocr-3B:

$$\begin{aligned}
-a^{ij}w_{x_i x_j} &= \frac{-a^{ij}u_{x_i x_j}v + a^{ij}v_{x_i x_j}u}{v^2} + \frac{a^{ij}v_{x_i}u_{x_j} - a^{ij}u_{x_i}v_{x_j}}{v^2} - a^{ij}\frac{2}{v}v_{x_j}\frac{v_{x_i}u - vu_{x_i}}{v^2} \\
&= \frac{(Lu - b^i u_{x_i} - cu)v + (-Lv + b^i v_{x_i} + cv)u}{v^2} + 0 + a^{ij}\frac{2}{v}v_{x_j}w_{x_i}, \text{ since } a^{ij} = a^{ji}. \quad (1)
\end{aligned}$$

$$= \frac{Lu}{v} - \frac{uLv}{v^2} - b^i w_{x_i} + a^{ij}\frac{2}{v}v_{x_j}w_{x_i} \quad (2)$$

$$= \frac{Lu}{v} - \frac{uLv}{v^2} - b^i w_{x_i} + a^{ij}\frac{2}{v}v_{x_j}w_{x_i} \quad (3)$$

Nanonets-OCR2-3B:

$$\begin{aligned}
-a^{ij}w_{x_i x_j} &= \frac{-a^{ij}u_{x_i x_j}v + a^{ij}v_{x_i x_j}u}{v^2} + \frac{a^{ij}v_{x_i}u_{x_j} - a^{ij}u_{x_i}v_{x_j}}{v^2} - a^{ij}\frac{2}{v}v_{x_j}\frac{v_{x_i}u - vu_{x_i}}{v^2} \\
&= \frac{(Lu - b^i u_{x_i} - cu)v + (-Lv + b^i v_{x_i} + cv)u}{v^2} + 0 + a^{ij}\frac{2}{v}v_{x_j}w_{x_i}, \text{ since } a^{ij} = a^{ji}.
\end{aligned}$$

DeepSeek-OCR-3B :

$$\begin{aligned}
-a^{ij}w_{x_i x_j} &= \frac{-a^{ij}u_{x_i x_j}v + a^{ij}v_{x_i x_j}u}{v^2} + \frac{a^{ij}v_{x_i}u_{x_j} - a^{ij}u_{x_i}v_{x_j}}{v^2} - a^{ij}\frac{2}{v}v_{x_j}\frac{v_{x_i}u - vu_{x_i}}{v^2} \\
&= \frac{(Lu - b^i u_{x_i} - cu)v + (-Lv + b^i v_{x_i} + cv)u}{v^2} + 0 + a^{ij}\frac{2}{v}v_{x_j}w_{x_i}, \text{ since } a^{ij} = a^{ji}. \\
&= \frac{Lu}{v} - \frac{uLv}{v^2} - b^i w_{x_i} + a^{ij}\frac{2}{v}v_{x_j}w_{x_i}
\end{aligned}$$

Figure 8 Results for a multi-line formula example. UniRec-0.1B, MonkeyOCR, and Nanonets-OCR2 produce fully correct results. Dolphin-1.5, MinerU2.5, and PaddleOCR-VL incorrectly classify the plain text word “since” as a formula style, and PaddleOCR-VL also fails to detect the correct line breaks. dots.ocr hallucinates a non-existent formula index. DeepSeek-OCR recognizes most of the content correctly but fails to recover the fraction at the end of the first line.

Label:

你可能最近看到了一则关于Tom Hanks推销牙科服务的广告。其实这位演员本人并没有参与拍摄。有人仅仅使用了他的肖像图片，结合深度伪造技术，就让他看起来参与了广告拍摄 \$ ^{1} \$ 。

UniRec-0.1B:

可能最近看到了一则关于Tom Hanks推销牙科服务的广告。其实这位演员本人并没有参与拍摄。有人仅仅使用了他的肖像图片，结合深度伪造技术，就让他看起来参与了广告拍摄¹。

Dolphin-1.5-0.3B:

你不知道,我们要做什么事。

PaddleOCR-VL-0.9B:

可能最近看到了一则关于 Tom Hanks 推销牙科服务的广告。其实这位演员本人并没有参与拍摄。有人仅仅使用了他的肖像图片，结合深度伪造技术，就让他看起来参与了广告拍摄 \$ ^{1} \$ 。

MinerU2.5 -1.2B:

你 可能最近看到了一则关于Tom Hanks推销牙科服务的广告。其实这位演员本人并没有参与拍摄。有人仅仅使用了他的肖像图片，结合深度伪造技术，就让他看起来参与了广告拍摄。

你

可能最近看到了一则关于 Tom Hanks 推销牙科服务的广告。其实这位演员本人并没有参与拍摄。有人仅仅使用了他的肖像图片，结合深度伪造技术，就让他看起来参与了广告拍摄¹。

Label:

\$ ^{1} \$ Sales-weighted, currency-adjusted composites \$ ^{2} \$ Compound annual growth rate

UniRec-0.1B:

1 Sales-weighted, currency-adjusted composites
2 Compound annual growth rate<|sn|>

Dolphin-1.5-0.3B:

1 Sales-weighted, currency-adjusted composites
2 Compound annual growth rate

PaddleOCR-VL-0.9B:

\$ ^{1} \$ Sales-weighted, currency-adjusted composites
\$ ^{2} \$ Compound annual growth rate

MinerU2.5 -1.2B:

1 Sales-weighted, currency-adjusted composites 2 Compound annual growth rate

MonkeyOCR-pro-3B:

可能最近看到了一则关于 Tom Hanks 推销牙科服务的广告。其实这位演员本人并没有参与拍摄。有人仅仅使用了他的肖像图片，结合深度伪造技术，就让他看起来参与了广告拍摄\$ ^{1} \$。

dots.ocr-3B:

你

可能最近看到了一则关于Tom Hanks推销牙科服务的广告。其实这位演员本人并没有参与拍摄。有人仅仅使用了他的肖像图片，结合深度伪造技术，就让他看起来参与了广告拍摄¹。

Nanonets-OCR2-3B:

你可能最近看到了一则关于Tom Hanks推销牙科服务的广告。其实这位演员本人并没有参与拍摄。有人仅仅使用了他的肖像图片，结合深度伪造技术，就让他看起来参与了广告拍摄₁。

DeepSeek-OCR-3B :

你

可能最近看到了一则关于 Tom Hanks 推销牙科服务的广告。其实这位演员本人并没有参与拍摄。有人仅仅使用了他的肖像图片，结合深度伪造技术，就让他看起来参与了广告拍摄₁。

1 Sales-weighted, currency-adjusted composites

2 Compound annual growth rate

MonkeyOCR-pro-3B:

\$ ^{1} \$ Sales\–weighted, currency\–adjusted composites \$ ^{2} \$ Compound annual growth rate

dots.ocr-3B:

1 Sales\–weighted, currency\–adjusted composites

2 Compound annual growth rate

Nanonets-OCR2-3B:

¹ Sales\–weighted, currency\–adjusted composites
² Compound annual growth rate

DeepSeek-OCR-3B :

1 Sales\–weighted, currency\–adjusted composites

2 Compound annual growth rate

Figure 9 Results for two failure cases of UniRec-0.1B. The model frequently predicts subscripts and superscripts outside mathematical contexts as plain text. This issue stems from our PyMuPDF-based training data extraction, which represents subscript and superscript elements as plain text. **Red characters** indicate recognition errors and **_** indicate missed characters. **Green** indicates correct recognition.

Document Image

10. *Proof.* We omit (a) since is standard. For (b), if u attains an interior maximum, then the conclusion follows from strong maximum principle.

If not, then for some $x^0 \in \partial U$, $u(x^0) > u(x) \forall x \in U$. Then Hopf's lemma implies $\frac{\partial u}{\partial \nu}(x^0) > 0$, which is a contradiction. \square

Remark 2. A generalization of this problem to mixed boundary conditions is recorded in *Gilbarg-Trudinger, Elliptic PDEs of second order, Problem 3.1*.

11. *Proof.* Define

$$B[u, v] = \int_U \sum_{i,j} a^{ij} u_{x_i} v_{x_j} dx \text{ for } u \in H^1(U), v \in H_0^1(U).$$

By Exercise 5.17, $\phi(u) \in H^1(U)$. Then, for all $v \in C_c^\infty(\bar{U})$, $v \geq 0$,

$$\begin{aligned} B[\phi(u), v] &= \int_U \sum_{i,j} a^{ij} (\phi(u))_{x_i} v_{x_j} dx \\ &= \int_U \sum_{i,j} a^{ij} \phi'(u) u_{x_i} v_{x_j} dx, (\phi'(u) \text{ is bounded since } u \text{ is bounded}) \\ &= \int_U \sum_{i,j} a^{ij} u_{x_i} (\phi'(u)v)_{x_j} - \sum_{i,j} a_{ij} \phi''(u) u_{x_i} u_{x_j} v dx \\ &\leq 0 - \int_U \phi''(u) v |Du|^2 dx \leq 0, \text{ by convexity of } \phi. \end{aligned}$$

(We don't know whether the product of two H^1 functions is weakly differentiable. This is why we do not take $v \in H_0^1$.) Now we complete the proof with the standard density argument. \square

12. *Proof.* Given $u \in C^2(U) \cap C(\bar{U})$ with $Lu \leq 0$ in U and $u \leq 0$ on ∂U . Since \bar{U} is compact and $v \in C(\bar{U})$, $v \geq c > 0$. So $w := \frac{u}{v} \in C^2(U) \cap C(\bar{U})$. Brutal computation gives us

$$\begin{aligned} -a^{ij} w_{x_i x_j} &= -a^{ij} u_{x_i x_j} v + a^{ij} v_{x_i} u_{x_j} + \frac{a^{ij} u_{x_i} u_{x_j} - a^{ij} u_{x_i} v u_{x_j} - a^{ij} v_{x_i} u u_{x_j}}{v^2} \\ &= \frac{(Lu - b^i u_{x_i} - cu)v + (-Lv + b^i v_{x_i} + cv)u + 0 + a^{ij} \frac{2}{v} v_{x_j} w_{x_i}}{v^2}, \text{ since } a^{ij} = a^{ji}. \\ &= \frac{Lu - uLv}{v} - b^i w_{x_i} + a^{ij} \frac{2}{v} v_{x_j} w_{x_i} \end{aligned}$$

Therefore,

$$Mw := -a^{ij} w_{x_i x_j} + w_{x_i} \left[b^i - a^{ij} \frac{2}{v} v_{x_j} \right] = \frac{Lu}{v} - \frac{uLv}{v^2} \leq 0 \text{ on } \{x \in \bar{U} : u > 0\} \subseteq U$$

If $\{x \in \bar{U} : u > 0\}$ is not empty, Weak maximum principle to the operator M with bounded coefficients (since $v \in C^1(\bar{U})$) will lead a contradiction that

$$0 < \max_{\{u>0\}} w = \max_{\partial\{u>0\}} w = \frac{0}{v} = 0$$

Hence $u \leq 0$ in U . \square

6

PaddleOCR-VL-0.9B

10. *Proof.* We omit (a) since is standard. For (b), if u attains an interior maximum, then the conclusion follows from strong maximum principle.

If not, then for some $x^0 \in \partial U$, $u(x^0) > u(x) \forall x \in U$. Then Hopf's lemma implies $\frac{\partial u}{\partial \nu}(x^0) > 0$, which is a contradiction.

Remark 2. A generalization of this problem to mixed boundary conditions is recorded in *Gilbarg-Trudinger, Elliptic PDEs of second order, Problem 3.1*.

11. *Proof.* Define

$$B[u, v] = \int_U \sum_{i,j} a^{ij} u_{x_i} v_{x_j} dx \text{ for } u \in H^1(U), v \in H_0^1(U).$$

By Exercise 5.17, $\phi(u) \in H^1(U)$. Then, for all $v \in C_c^\infty(\bar{U})$, $v \geq 0$,

$$\begin{aligned} B[\phi(u), v] &= \int_U \sum_{i,j} a^{ij} (\phi(u))_{x_i} v_{x_j} dx \\ &= \int_U \sum_{i,j} a^{ij} \phi'(u) u_{x_i} v_{x_j} dx, (\phi'(u) \text{ is bounded since } u \text{ is bounded}) \\ &= \int_U \sum_{i,j} a^{ij} u_{x_i} (\phi'(u)v)_{x_j} - \sum_{i,j} a_{ij} \phi''(u) u_{x_i} u_{x_j} v dx \\ &\leq 0 - \int_U \phi''(u) v |Du|^2 dx \leq 0 \text{ by convexity of } \phi. \end{aligned}$$

(We don't know whether the product of two H^1 functions is weakly differentiable. This is why we do not take $v \in H_0^1$.) Now we complete the proof with the standard density argument. \square

12. *Proof.* Given $u \in C^2(U) \cap C(\bar{U})$ with $Lu \leq 0$ in U and $u \leq 0$ on ∂U . Since \bar{U} is compact and $v \in C(\bar{U})$, $v \geq c > 0$. So $w := \frac{u}{v} \in C^2(U) \cap C(\bar{U})$. Brutal computation gives us

$$\begin{aligned} -a^{ij} w_{x_i x_j} &= -a^{ij} u_{x_i x_j} v + a^{ij} v_{x_i} u_{x_j} + \frac{a^{ij} u_{x_i} u_{x_j} - a^{ij} u_{x_i} v u_{x_j} - a^{ij} v_{x_i} u u_{x_j}}{v^2} \\ &= \frac{(Lu - b^i u_{x_i} - cu)v + (-Lv + b^i v_{x_i} + cv)u + 0 + a^{ij} \frac{2}{v} v_{x_j} w_{x_i}}{v^2}, \text{ since } a^{ij} = a^{ji}. \\ &= \frac{Lu - uLv}{v} - b^i w_{x_i} + a^{ij} \frac{2}{v} v_{x_j} w_{x_i} \end{aligned}$$

Therefore,

$$Mw := -a^{ij} w_{x_i x_j} + w_{x_i} \left[b^i - a^{ij} \frac{2}{v} v_{x_j} \right] = \frac{Lu}{v} - \frac{uLv}{v^2} \leq 0 \text{ on } \{x \in \bar{U} : u > 0\} \subseteq U$$

If $\{x \in \bar{U} : u > 0\}$ is not empty, Weak maximum principle to the operator M with bounded coefficients (since $v \in C^1(\bar{U})$) will lead a contradiction that

$$0 < \max_{\{u>0\}} w = \max_{\partial\{u>0\}} w = \frac{0}{v} = 0$$

Hence $u \leq 0$ in U .

Figure 10 Results for a page-level example with mixed text and formal content. PaddleOCR-VL and MinerU2.5 misclassify plain text embedded in mathematical expressions as formulas, whereas UniRec-0.1B correctly identifies them as text.

UniRec-0.1B

10. *Proof.* We omit (a) since is standard. For (b), if u attains an interior maximum, then the conclusion follows from strong maximum principle.

If not, then for some $x^0 \in \partial U$, $u(x^0) > u(x) \forall x \in U$. Then Hopf's lemma implies $\frac{\partial u}{\partial \nu}(x^0) > 0$, which is a contradiction. \square

Remark 2. A generalization of this problem to mixed boundary conditions is recorded in *Gilbarg-Trudinger, Elliptic PDEs of second order, Problem 3.1*.

11. *Proof.* Define

$$B[u, v] = \int_U \sum_{i,j} a^{ij} u_{x_i} v_{x_j} dx \text{ for } u \in H^1(U), v \in H_0^1(U).$$

By Exercise 5.17, $\phi(u) \in H^1(U)$. Then, for all $v \in C_c^\infty(\bar{U})$, $v \geq 0$,

$$\begin{aligned} B[\phi(u), v] &= \int_U \sum_{i,j} a^{ij} (\phi(u))_{x_i} v_{x_j} dx, (\phi'(u) \text{ is bounded since } u \text{ is bounded}) \\ &= \int_U \sum_{i,j} a^{ij} u_{x_i} (\phi'(u)v)_{x_j} - \sum_{i,j} a_{ij} \phi''(u) u_{x_i} u_{x_j} v dx \\ &\leq 0 - \int_U \phi''(u) v |Du|^2 dx \leq 0, \text{ by convexity of } \phi. \end{aligned}$$

(We don't know whether the product of two H^1 functions is weakly differentiable. This is why we do not take $v \in H_0^1$.) Now we complete the proof with the standard density argument. \square

12. *Proof.* Given $u \in C^2(U) \cap C(\bar{U})$ with $Lu \leq 0$ in U and $u \leq 0$ on ∂U . Since \bar{U} is compact and $v \in C(\bar{U})$, $v \geq c > 0$. So $w := \frac{u}{v} \in C^2(U) \cap C(\bar{U})$. Brutal computation gives us

$$\begin{aligned} -a^{ij} w_{x_i x_j} &= -a^{ij} u_{x_i x_j} v + a^{ij} v_{x_i} u_{x_j} + \frac{a^{ij} u_{x_i} u_{x_j} - a^{ij} u_{x_i} v u_{x_j} - a^{ij} v_{x_i} u u_{x_j}}{v^2} \\ &= \frac{(Lu - b^i u_{x_i} - cu)v + (-Lv + b^i v_{x_i} + cv)u + 0 + a^{ij} \frac{2}{v} v_{x_j} w_{x_i}}{v^2}, \text{ since } a^{ij} = a^{ji}. \\ &= \frac{Lu - uLv}{v} - b^i w_{x_i} + a^{ij} \frac{2}{v} v_{x_j} w_{x_i} \end{aligned}$$

Therefore,

$$Mw := -a^{ij} w_{x_i x_j} + w_{x_i} \left[b^i - a^{ij} \frac{2}{v} v_{x_j} \right] = \frac{Lu}{v} - \frac{uLv}{v^2} \leq 0 \text{ on } \{x \in \bar{U} : u > 0\} \subseteq U$$

If $\{x \in \bar{U} : u > 0\}$ is not empty, Weak maximum principle to the operator M with bounded coefficients (since $v \in C^1(\bar{U})$) will lead a contradiction that

$$0 < \max_{\{u>0\}} w = \max_{\partial\{u>0\}} w = \frac{0}{v} = 0$$

Hence $u \leq 0$ in U .

MinerU2.5-1.2B

10. *Proof.* We omit (a) since is standard. For (b), if u attains an interior maximum, then the conclusion follows from strong maximum principle.

If not, then for some $x^0 \in \partial U$, $u(x^0) > u(x) \forall x \in U$. Then Hopf's lemma implies $\frac{\partial u}{\partial \nu}(x^0) > 0$ which is a contradiction.

Remark 2. A generalization of this problem to mixed boundary conditions is recorded in *Gilbarg-Trudinger, Elliptic PDEs of second order, Problem 3.1*.

11. *Proof.* Define

$$B[u, v] = \int_U \sum_{i,j} a^{ij} u_{x_i} v_{x_j} dx \text{ for } u \in H^1(U), v \in H_0^1(U).$$

By Exercise 5.17, $\phi(u) \in H^1(U)$. Then, for all $v \in C_c^\infty(\bar{U})$, $v \geq 0$,

$$\begin{aligned} B[\phi(u), v] &= \int_U \sum_{i,j} a^{ij} (\phi(u))_{x_i} v_{x_j} dx, (\phi'(u) \text{ is bounded since } u \text{ is bounded}) \\ &= \int_U \sum_{i,j} a^{ij} u_{x_i} (\phi'(u)v)_{x_j} - \sum_{i,j} a_{ij} \phi''(u) u_{x_i} u_{x_j} v dx \\ &\leq 0 - \int_U \phi''(u) v |Du|^2 dx \leq 0 \text{ by } \boxed{\text{by convexity of } \phi}. \end{aligned}$$

(We don't know whether the product of two H^1 functions is weakly differentiable. This is why we do not take $v \in H_0^1$.) Now we complete the proof with the standard density argument.

12. *Proof.* Given $u \in C^2(U) \cap C(\bar{U})$ with $Lu \leq 0$ in U and $u \leq 0$ on ∂U . Since \bar{U} is compact and $v \in C(\bar{U})$, $v \geq c > 0$. So $w := \frac{u}{v} \in C^2(U) \cap C(\bar{U})$. Brutal computation gives us

$$\begin{aligned} -a^{ij} w_{x_i x_j} &= -a^{ij} u_{x_i x_j} v + a^{ij} v_{x_i} u_{x_j} + \frac{a^{ij} u_{x_i} u_{x_j} - a^{ij} u_{x_i} v u_{x_j} - a^{ij} v_{x_i} u u_{x_j}}{v^2} \\ &= \frac{(Lu - b^i u_{x_i} - cu)v + (-Lv + b^i v_{x_i} + cv)u + 0 + a^{ij} \frac{2}{v} v_{x_j} w_{x_i}}{v^2}, \text{ since } a^{ij} = a^{ji}. \\ &= \frac{Lu - uLv}{v} - b^i w_{x_i} + a^{ij} \frac{2}{v} v_{x_j} w_{x_i} \end{aligned}$$

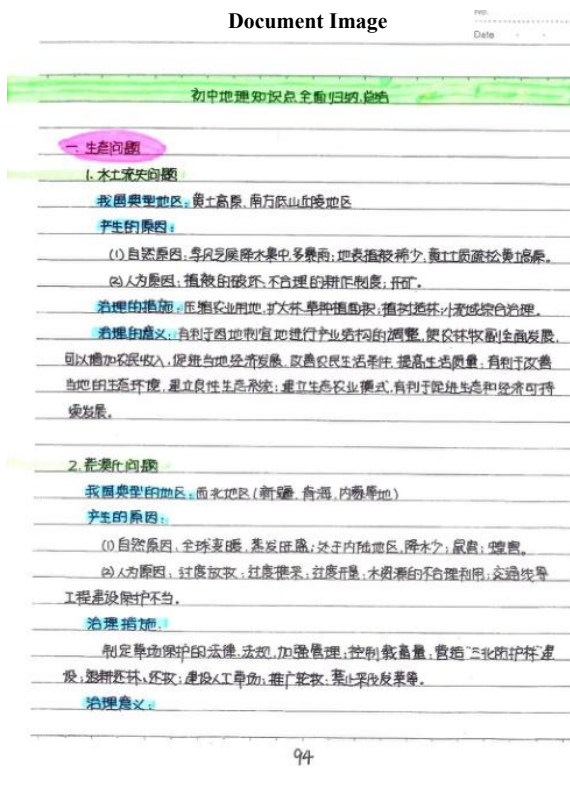
Therefore,

$$Mw := -a^{ij} w_{x_i x_j} + w_{x_i} \left[b^i - a^{ij} \frac{2}{v} v_{x_j} \right] = \frac{Lu}{v} - \frac{uLv}{v^2} \leq 0 \text{ on } \{x \in \bar{U} : u > 0\} \subseteq U$$

If $\{x \in \bar{U} : u > 0\}$ is not empty, Weak maximum principle to the operator M with bounded coefficients (since $v \in C^1(\bar{U})$) will lead a contradiction that

$$0 < \max_{\{u>0\}} w = \max_{\partial\{u>0\}} w = \frac{0}{v} = 0$$

Hence $u \leq 0$ in U .



94

PaddleOCR-VL-0.9B

初中地理知识点全面归纳总结

一. 生态问题

1. 水土流失问题

我国典型地区：黄土高原，南方低山丘陵地区

产生的原因：

(1) 自然原因：季风气候降水集中，多暴雨；地表植被稀少；黄土土质疏松，易受冲刷。

(2) 人为原因：植被的破坏，不合理的耕作制度；开矿。

治理的措施：压缩农业用地，扩大林草种植面积；植树造林；~~河流~~流域综合治理。

治理的意义：有利于因地制宜地进行产业结构的调整，使农林牧副全面发展，可以增加农民收入，促进当地经济发展，改善农民生活条件，提高生活质量；有利于改善当地的生态环境，建立良性生态系统；建立生态农业模式，有利于促进生态和经济可持续发展。

2. 荒漠化问题

我国典型的地区：西北地区（新疆、青海、内蒙古等地）

产生的原因：

(1) 自然原因：全球变暖，蒸发旺盛；处于内陆地区，降水少；鼠害；蝗害。

(2) 人为原因：过度放牧；过度樵采；过度开垦；水资源的不合理利用；交通线等工程建设保护不当。

治理措施：

制定草场保护的法律、法规，加强管理；控制载畜量；营造“三北防护林”建设；退耕还林、还牧；建设人工草场；推广轮牧；禁止采伐发菜等。

治理意义：

UniRec-0.1B

初中地理知识点全面归纳、总结

一. 生态问题

1. 水土流失问题

我国典型地区：黄土高原、南方低山丘陵地区

产生的原因：

(1) 自然原因：季风气候降水集中，多暴雨；地表植被稀少；黄土土质疏松，易受冲刷。

(2) 人为原因：植被的破坏，不合理的耕作制度；开矿。

治理的措施：压缩农业用地，扩大林草种植面积；植树造林；小流域综合治理。

治理的意义：有利于因地制宜地进行产业结构的调整，使农林牧副全面发展，可以增加农民收入，促进当地经济发展，改善农民生活条件，提高生活质量；有利于改善当地的生态环境，建立良性生态系统；建立生态农业模式，有利于促进生态和经济可持续发展。

2. 荒漠化问题

我国典型的地区：西北地区（新疆、青海、内蒙古等地）

产生的原因：

(1) 自然原因：全球变暖，蒸发旺盛；处于内陆地区，降水少；鼠害；蝗害。

(2) 人为原因：过度放牧；过度樵采；过度开垦；水资源的不合理利用；交通线等工程建设保护不当。

治理措施：

制定草场保护的法律、法规，加强管理；控制载畜量；营造“三北防护林”建设；退耕还林、还牧；建设人工草场；推广轮牧；禁止采伐发菜等。

治理意义：

MinerU2.5-1.2B

初中地理知识点全面归纳总结

一. 生产问题

1. ~~土壤~~流失问题

我国典型地区：黄土高原，南方低山丘陵地区

产生的原因：

(1) 自然原因：~~季~~风气候降水集中，多暴雨；地表植被稀少；黄土土质疏松，易受冲刷。

(2) 人为原因：植被的破坏，不合理的耕作制度；开矿。

治理的措施：压缩农业用地，扩大林草种植面积；植树造林；小流域综合治理。

治理的意义：有利于因地制宜地进行产业结构的调整，使农林牧副全面发展，可以增加农民收入，促进当地经济发展，改善农民生活条件，提高生活质量；有利于改善当地的生态环境，建立良性生态系统；建立生态农业模式，有利于促进生态和经济可持续发展。

2. 荒漠化问题

我国典型的地区：西北地区（新疆、青海、内蒙古等地）

产生的原因：

(1) 自然原因：全球变暖，蒸发旺盛；处于内陆地区，降水少；鼠害；~~蝗~~害。

(2) 人为原因：过度放牧；过度樵采；过度开垦；~~水~~资源的不合理利用；交通线等

工程建设保护不当。

治理措施：

制定草场保护的法律、法规，加强管理；控制载畜量；营造“三北防护林”建设；退耕还林、还牧；建设人工草场；推广轮牧；禁止采伐~~及~~发菜等。

治理意义：

Figure 11 Results for a page-level case with handwritten content. PaddleOCR-VL misidentifies “小流” as “河流,” likely due to overreliance on linguistic context, while most errors in MinerU 2.5 arise from homophones.